Scientific report; WR-2002-07

KNMI

Effect of aerosols on UV-index

Jordi Bacoa and Michiel van Weele

De Bilt, 2002

Scientific report = Wetenschappelijk Rapport; WR 2002-07

De Bilt, 2002

PO Box 201, 3730 AE De Bilt
The Netherlands
Wilhelminalaan 10
http://www.knmi.nl
Telephone +31 30 22 06 911
Telefax +31 30 22 10 407

Authors: Jordi Badosa
Michiel van Weele

UDC: 551.510.42
551.501.721
551.521.17

ISSN: 0169-1651

ISBN: 90-369-2222-4

e f e i o a e
o n u v i x

Jordi Badosa Michiel van Weele

KNMI, De Bilt, December 2002

This report contains the main results obtained during a 3 months (August-November 2002) stage at KNMI (De Bilt)

Deze publikatie is mede tot stand gekomen dankzij door het NIVR gefinancierd werk

Index

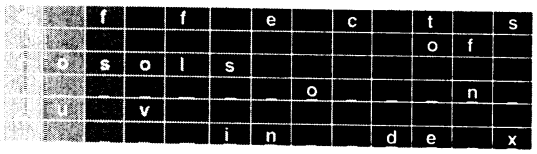

1 Introduction

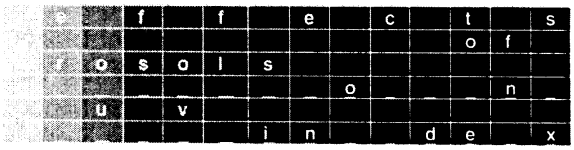

The UV radiation (200-400 nm) reaching the top of the atmosphere from the Sun is about 8% of the total solar radiation (39% is in the visible band and 53% belongs to the infrared). When considering the amount of UV radiation on the Earth surface, the percentage is even smaller due to the strong absorption experimented by the atmospheric constituents, above all ozone. However, this little portion of radiation plays a decisive role in atmospheric chemistry, is necessary for life and, in extreme amounts, it can also create a lot of damage to living beings.

Because of this potential damage UV radiation in the atmosphere has been widely studied since the 80s, when the ozone depletion in some parts of the planet and the associated increase in the UV levels were discovered.

Many organisations were created, institutions joined efforts and a lot of research groups exclusively dedicated to the study of this kind of radiation appeared, designing and improving the instrumentation, studying the biological effects of the UV radiation and also generating information to advise the population about the UV risks. In this sense, the Australians were the firsts to make education campaigns and warn against harmful UV levels through the media. In 1987, New Zealand began prevention campaigns and, in 1992, a UV index (ranging between 0 and 10) was defined in Canada and predictions of this index were daily distributed. United States elaborated a similar index.

Nowadays, a unique definition of the UV Index is accepted and used by the science community, and this will be the magnitude of study of this report.

This chapter introduces the UV radiation, defines the UV Index (UVI) (1₁) and identifies the main environmental factors affecting the UV radiation, with special attention to aerosols (1₂).

1₁ UV Radiation & UV Index (UVI) ←

The UV radiation (200-400 nm) is usually discomposed into three ranges, depending on their biological effect: UVC (200-280 nm), UVB (280-320 nm) and UVA (320-400) nm[1]. The whole UVC radiation and most of UVB are absorbed in the upper atmosphere mainly by ozone and oxygen molecules. It is very important that these two types of radiation don't reach the surface because these could cause great damage (even the death) to living beings. Actually, if it did reach the ground, life as we know it wouldn't be possible.

Many negative effects derived from exposition to UV radiation have been discovered, but it also has some benefits necessary for life. For human beings, UV radiation plays a decisive roll in the vitamin-D synthesis on the skin. The most important harmful effects of UV radiation on humans are the erythema (or sunburn), cornea affections, and skin cancers, mainly produced by the UVB radiation, and skin aging, loose of elasticity of the skin and crystalline affections, which UVA is responsible for.

[1] There is some controversies in UVB and UVA definition. According to the *Comission Internationale de l'Eclairage* (CIE) and the COST-713 action, these bands are defined from 280 to 315 nm and from 315 to 400 nm, respectively. However, the World Meteorological Organization (WMO) and many authors use the definition considered here. Actually, this report will not focus on the study of the UVB and UVA radiation separately (our magnitude of study is the UV Index), but, as also pointed by Krupa *et al* (1998), we don't expect discontinuities in the biological responses between 315 and 320 nm.

During the second half of the 20th century, a lot of cases of skin cancer and cataracts appeared, not only because of the increase of UV radiation (caused by the decline of stratospheric ozone), but also due to the change in the habits of the people. In the beginning of the 20th century, having a white skin was a social status symbol but with the arrival of the holidays and the practice of going to the beach, the tanned skins began to be very desirable. This, together with the evolution of the fashion to less covering clothes, made the exposition of the skin to the UV radiation greatly increase and, as a consequence, so did the diseases risks. Australia, New Zealand and Canada are some of the countries where it has appeared more cases of skin cancer and cataracts. This is since mostly English and French inhabited these countries in the colonization time, with a whiter skin than the native original people and, therefore, with less protection to the higher UV exposition registered there. In order to advise and warn the population about the risks of the UV radiation, these three countries began to diffuse information through the media and give some simple indices that represented the maximum UV level expected for the next day. This was the embryo of the nowadays accepted UV Index.

The UV Index (UVI) is an estimation of the UV levels that are important for the effects on the human skin. UVI is an artificial quantity derived from the erythemal irradiance, which is the integration of the monochromatic UV irradiance (280-400 nm) weighted by the CIE (*Comission Internacionale de l'Eclairage*) spectral action function (McKinlay & Diffey, 1987). Figure 1.1 shows the CIE function together with an example spectrum (typical for a summer noon at midlatitudes) and the result of their multiplication. As it is seen, the energy is weighted such for the erythemal irradiance, that UVB is much more important than UVA. For the global irradiance, 94% (about 52 W/m^2, in this case) of the energy corresponds to UVA and only 6% (about 3 W/m^2) belongs to UVB; on the other hand, in the erythemal irradiance, 83% of the effect is in the UVB range while only 17% is in the UVA. These numbers show the important role of the UVB radiation although it constitutes less than 0.1% of the total irradiance coming from the Sun to the Earth surface. The erythemal irradiance represents about 0.02% of the total irradiance (Lorente et al, 1994). This gives evidence that small changes in UVB can imply strong biological effects and also that very precise instruments are needed to measure this radiation.
The UVI value is found multiplying the erythemal irradiance by 40 and it is usually rounded to the closest integer. UVI commonly takes values from 0 to 16 (reaching the maximum in summer) but in some regions and seasons it can be quite larger (*e.g.* up to 20 in Australia). Although one can consider an instantaneous value, at first the UVI was defined as the maximum daily-predicted value. However, the current use of this index has been widened and it makes sense to refer to the evolution of the measured and predicted UVI during the day.
A daily noon forecast of the UVI index for the entire world is retrieved by the GOME fast delivery centre, which is integrated by researchers of KNMI and elaborate some products from the GOME (Global Ozone Monitoring Experiment) instrument on board of ERS-2 satellite of the ESA. The UV forecasts are delivered to the public in the framework of the DUP (Data User Program) of ESA. The UVI calculations are made with an empirical algorithm for clear skies that has two input parameters: the total ozone column (TOZ) and the solar zenith angle (SZA) (Allaart et al, 2002). Additional corrections are applied for the elevation of the surface and for the Earth-Sun distance, which varies with season. Representations of UVI forecasts for the following 5 days and also the values for any site can be consulted in Internet (www.knmi.nl/gome_fd).

Figure 1.1 Representation of one spectrum of global irradiance and the CIE function (left) and the result of their multiplication (right). The integration of this curve gives the erythemal irradiance.

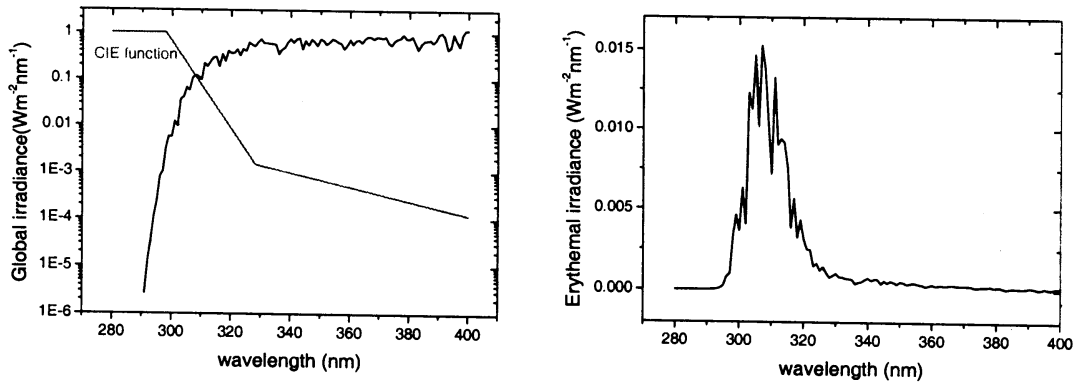

1.2 Main Factors Affecting the UV Radiation ←

The main factors that affect the UV radiation (and UVI) since it enters the atmosphere and until it reaches the ground are solar zenith angle (SZA), ozone, clouds, surface albedo, aerosols and altitude. We briefly comment the effects of all these factors, with special attention to aerosols:

SZA

SZA is defined as the angle between the solar and the zenith direction. It affects both the angular distribution of the solar radiation and the optical path through the atmosphere. As SZA increases, the radiation has to go through a thicker atmosphere and, therefore, the effects of some constituents like ozone and aerosols become more important. Actually, SZA is the main factor that affects UV radiation, leading to a reduction of about 17% when SZA varies from 0 to 60 degrees and to about 0.4 % when reaching 85 degrees (Badosa, 2002).
SZA can be easily calculated using well known Sun-Earth geometry formulas given the day, time and the latitude and longitude of the site of interest (*e.g.* Iqbal, 1983, Lenoble, 1993).

TOZ

The most important parameter for the effect of ozone on UV radiation is the total ozone column (TOZ) defined as the thickness that the column of ozone would have if it had standard temperature and pressure (0 deg C and 1 atm). The natural units are atm-cm but it is more commonly used the so-called Dobson Units (DU) defined as 1 atm-cm = 1000 DU; 1 DU of ozone corresponds to 2.69 10^{20} molecules per m^2 in an ozone column.
As commented above, ozone strongly absorbs the UV radiation such that UVC and most of UVB do not reach the surface. This absorption has a large wavelength dependence in the UVB range in such a way that, for midlatitudes, a 10% reduction in TOZ involves about 2% of increase in the surface UV irradiance at 320 nm while at 290 nm the change is approximately of 110% (Ziemke *et al*, 1998). One can explain in a simple way the changes on UVI when TOZ varies by means of the Radiation Amplification Factor (RAF), which is defined as the percentage of variation in UVI when TOZ is reduced by 1%. The COST-713 Action experts group (which redacted a guide for the UVI forecast) set RAF between 1.1 and 1.3 (Vanicek *et al*, 2000). That means that a reduction of 10% in TOZ causes an increase in UVI between 11 and 13 %.

CLOUDS

The study of the effects of clouds on UVI is complex due to the great temporal and spatial variability of cloud parameters and the difficulties to characterize their optical properties. However, it is known that clouds can induce both an increase and decrease in UVI. For example, Tunc (1999) found enhancements of 16% in UVI for broken clouds; Sabburg & Wong (2000) found, from UVB measurements, that 3 % of the cases showed enhancements up to 8%, mostly (in 86% of the cases) due to the presence of cirrus clouds or turbidity. The reduction effect is the most usual and is much larger; Renaud *et al* (2000) showed decreases in UVI to about 8% for thick clouds and 70% for thin clouds in overcast conditions. The COST-713 Action contemplated reductions down to 20% of the clear sky radiation (for overcast conditions and rain) (Vanicek *et al*, 2000) and the SUVDAMA (Scientific UV Data Management) project found, from UV spectral measurements, reductions down to 30% (Seckmeyer *et al*, 2000).

ALBEDO

The surface albedo is defined as the ratio between the reflected and the incident irradiance on a horizontal surface and depends on wavelength and the characteristics of the ground. For most of the surfaces the UV albedo is very small, typically about 2-5% (see Madronich *et al*, 1994, for examples). Sand (with a typical albedo of 0.3) and snow (up to 1 for fresh snow) are remarkable exceptions (e.g., Vanicek *et al*, 2000). Renaud *et al* (2000) found, for clear skies and snow conditions, enhancements of about 15 to 25% due to the multiple ground-atmosphere reflections. They also saw that this relative increment was about 80% larger for overcast conditions. The combined factors of snow and aerosols in cloudless situations can lead to enhancements in UVI of about 50% for moderately polluted atmospheres (Badosa, 2002).
It is also remarkable that the exposure on tilted or vertical surfaces to UV radiation can be doubled when the ground is covered by snow (*e.g.* Weihs *et al*, 2000).

ALTITUDE

UV radiation increases with altitude because the overlying atmosphere thickness diminishes and, therefore, also its extinction. Frederick (1993) found through modelling an increase of 6% per km while Blumthaler *et al* (1992, 1994) found much larger values, 15-18% per km, from direct-Sun measurements in the Alps (Long *et al*, 1996). The COST-713 Action, the UVI increases about 6-8% per km (Vanicek *et al*, 2000). Badosa et al (2002) showed, from modelling, enhancements of 5% per km for clear skies and low presence of aerosols for plain surfaces.
This wide range of effects observed give evidence that the altitude effect is a large-scale phenomenon and depends on the topography of the site, the air pollution and the albedo.

AEROSOLS

The aerosols scatter and absorb the UV radiation provoking the attenuation of the direct component and an increase of the diffuse. The global (direct + diffuse) irradiance is typically attenuated. Some remarkable exceptions are the snow-covered surfaces situations, as commented above.
The relationship between the incident extraterrestrial solar radiation (I_0) and the transmitted direct component (I) is explained by the Beer-Lambert law:

$$I = I_0 \exp(-\sum_i \tau_i(\lambda, z) \cdot m_i)$$

where τ_i and m_i are the optical depths and air masses of the different atmospheric components, among them also the aerosols. The aerosol optical depth (AOD) is the most important parameter to explain the effects of aerosols on UVI (e.g. Badosa *et al*, 2002). Other parameters that characterise the aerosol optical properties are the single scattering albedo (SSA) and the aerosol phase function. SSA is defined as

$$SSA = \sigma_s / (\sigma_s + \sigma_a)$$

where σ_s an σ_a are the cross sections for scattering and absorption, respectively. If SSA=1, the aerosol only scatters and if it is 0, it is a pure absorber. Typically, SSA ranges between 0.8 and 0.999 in the UV range (Madronich, 1993).
The phase function $P(\theta,\phi,\theta',\phi')$ is defined as the probability that a incident photon at the angles θ' and ϕ' is scattered into angles θ and ϕ. For molecular scattering (Rayleigh) the phase function is symmetric, i.e., with the same probability of back-scattering than forward-scattering; for aerosols this become more complicated. The forward-scattering is usually strong for larger aerosols. For radiative transfer purposes, the asymmetry factor (G) is used as a simplification of the phase function. G is defined as

$$G = \frac{1}{2}\int_{-1}^{1} P(\Theta)\cos(\Theta)d(\cos(\Theta))$$

and takes values from −1 (perfect back-scattering) to +1 (perfect forward-scattering) and is 0 for Rayleigh scattering. Typical values of G for aerosols range between 0.6 and 0.8 (Madronich, 1993).

Many studies have reported the attenuating effect of aerosols. From the SUVDAMA project measurements analyses, it was found that the global UV irradiance was reduced by 20% for aerosol optical depths from 0.1 to 1 at 355 nm (Seckmeyer *et al*, 2000). Lorente *et al* (1994) detected reductions of the UVB irradiance up to 14% and 37 % at 30 and 60 degrees of SZA, respectively, due to urban aerosols in Barcelona. Meleti & Capellani (2000), on basis of one year of aerosol optical depth and UV measurements at Ispra, detected maximum decreases in UVB of about 24% and 39% for these two values SZA. Reuder & Schwander (1999), identified, from modeling, reductions in UVI of 24% and 30% at 40 and 70 degrees, respectively, for a high-turbidity atmosphere with respect to a low-turbidity scenario. Wenny *et al* (2001) showed (combining aerosol measurements near Black Mountain, North Carolina, and modeling) that for strong absorption aerosols situations, UVI could be decreased by up to 5 units.

2 Objectives & Methodology

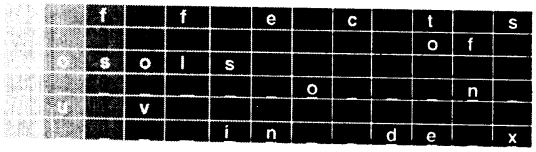

As seen in Chapter 1, aerosols can strongly affect the UV radiation reaching the Earth surface. Actually, aerosols produce larger effects in the UV band than in the other solar bands (visible and infrared) (e.g., Lorente *et al*, 1994). Over the last century, the presence of aerosols in the atmosphere has been increased on large scales mostly due to human activities. It has been estimated that the amount of UVB radiation has decreased between 5 and 18% since the industrial revolution (Liu *et al*, 1991). In relation with this, many authors have pointed out that the increasing effect of aerosols could have been partly or completely compensated by the UVB enhancement due to stratospheric ozone depletion (e.g. Reuder & Schwander, 1999). While the effect of ozone to UVI has been widely studied and is very well known, much less knowledge exists on the aerosols effects on UVI. This is because aerosols show large spatial and temporal variability, which makes it difficult to extrapolate their effects to global scales (e.g. Hänel, 1994).

Currently, most of UVI calculations for forecast applications consider constant aerosol properties. Wenny *et al* (2001) showed differences up to +4% and –50% between the UVI forecasts made by the USA National Weather Service compared with calculations that took into account the actual aerosol characteristics.

The present work contributes to the study of aerosol effects on UV Index. In this Chapter we present our objectives in this study (2₁) and the methodology that we have followed to reach these objectives (2₂).

2₁ Objectives ←

The ultimate goal of this work is to propose a simple parameterisation that explains the effects of aerosols on UVI and can be used world wide for forecasts or fast calculations purposes. This parameterisation has to be able to explain a wide range of atmospheric conditions and pollution scenarios. However, we will limit this to non-extremely amounts of aerosols, which are situations that only occur in very polluted cities, such as Mexico City.

Reaching this principal objective involves other secondary objectives that are also purposes of this work. The more evident one is to contribute to the knowledge of the aerosol effects on UVI, through a lot of tests performed for a wide range of conditions and a lot of representations of absolute and relative effects. In this way, this work categorises the importance of the most commonly used aerosol parameters concerning their contribution to the effect on UVI.

Also, this report will propose a parameterisation to calculate UVI that includes the aerosol parameterisation found.

Cloud-free conditions will be considered in this study due to the complexity of the study of the effect of clouds on UVI (as commented in Chapter 1). This inclusion would be another entire study.

Concerning surface albedo, we will not consider snow presence despite it has been explained in Chapter 1 that snow can produce, in combination with aerosols, enhancements of UV radiation. The situations with snow-covered surface also take place in mountain regions, where topography and surface elevation play an important role in combination with albedo effect, which make the effects at each site different. For the same reasons, the altitude effect will not be included in this work. Nevertheless, estimations, as given in Chapter 1, could be used.

2.2 Methodology ←

To reach the objectives we have applied the Troposphere Ultraviolet and Visible (TUV) radiative transfer model (Madronich et al, 2002) as a main tool of the study. All the knowledge learned about the aerosol effect on UVI in this work comes from calculations made with TUV model.
Chapter 3 introduces the main characteristics of this model and describes the considered aerosol optical parameters. This Chapter also presents the results of the sensitivity study of these parameters made with TUV in order to identify the most important parameters that affect UVI.
In Chapter 4, a parameterisation of the aerosol effects on UVI is searched, based on the results of the sensitivity study. An error analysis of this parameterisation is presented.
In Chapter 5, we present two algorithms to calculate UVI; the first one already existed, it is empirical and considers the aerosol presence in a climatological way. By fitting TUV calculations, we have derived a second algorithm, following the method used for the first, and considering the aerosol parameterisation obtained in Chapter 4. Chapter 5 also presents a first validation of our algorithm with measurements in De Bilt.
Chapter 6 summarizes our conclusions and mentions the possible steps to continue this work.

3 Sensitivity Study

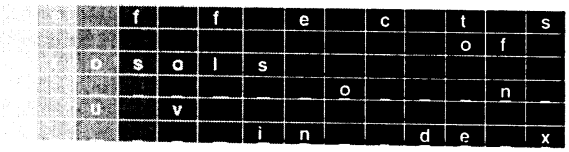

To completely describe the aerosol optical properties and to study their radiative effect, each wavelength and altitude level values of three parameters are needed: aerosol optical depth (AOD), single scattering albedo (SSA) and the aerosol phase function, which is in practice simplified by the asymmetry factor (G) (see Chapter 1 for definitions of these parameters). In this Chapter, we first introduce the TUV model (Madronich *et al*, 2002) with which we will do all UVI calculations and expose the main options selected for the calculations (also how we treat these three parameters) (3₁); then we present the results of our sensitivity study remarking which aerosol parameters are more important for their effect on UVI and deciding which ones take part in the parameterisation (3₂).

3₁ Modelling Conditions ←

The Tropospheric Ultraviolet & Visible (TUV) (Madronich *et al*, 2002) is a multi-layer model that considers two methods to solve the radiative transfer equation: two-stream and discrete ordinates (DISORT) with n streams; both methods can consider pseudo-spherical corrections. TUV can operate between 121 and 750 nm with a resolution definable by the user. It permits calculations of spectral irradiances (separating the direct and diffuse components), actinic fluxes, photodissociation coefficients and some pre-defined biologically effective irradiances, among them the UV Index. TUV considers aerosols and clouds and their properties are characterized for each working wavelength and each altitude level defined by the user. The code is in FORTRAN 77, and consists of a main program that calls peripheral functions that generate the profiles and parameters needed for the transfer calculations and it is very easy to change and personalise; it operates in UNIX environment. The TUV code is free and available through Internet (http:/www.acd.ucar.edu/TUV/).
For this study we have used TUV version 4.1. Table 3₁ highlights some conditions that we have considered (including the aerosol treatment) for all the calculations we will present in this report (the non mentioned conditions have been taken as default).

Table 3₁ Main conditions considered for all the UVI calculations with TUV model made in this work. The characteristics marked with D are set as default in TUV version 4.1

UV (200-400 nm) resolution		1 nm	D
Surface elevation		0 km	D
Altitude grid		0-80 km with 1 km resolution	D
UV (200-400 nm) extraterrestrial flux		from Atlas 3	D
Ozone absorption cross section temperature dependence		Bass & Paur (1986) polynomial function in the range 245-342 nm (reference at Madronich *et al*, 2002)	
Aerosols optical depth	altitude profile	½AOD in 0-1km and ½AOD in 1-2 km. For altitude>2 AOD=0	
	at each λ	using Ångström's formula (Ångström, 1961) from 368 nm	D
SSA and G		constant for each wavelength	D
Earth-Sun distance correction factor		1	
Surface albedo		0.05 (see discussion in Chapter 1)	
Radiative transfer code		pseudo-spherical two-streams (ps2str)	D

We used the two-stream radiative transfer code because it is much faster than DISORT and we needed to perform a lot of calculations. It is known that ps2str has some systematic errors, mostly for values of SZA close to 90 degrees. We estimate this error (from comparisons made with DISORT) typically to be less than 3%. Koepke et al (1998) studied the use of different models for the calculation of UVI.
Concerning the aerosol properties, we consider two layers (0-1km and 1-2km) with half of the total AOD contribution in each layer. No stratospheric aerosols are considered. We explain the AOD wavelength dependence through the Ångström's formula (Ångström, 1961)

$$AOD(\lambda) = \beta\lambda^{-\alpha} \qquad (31)$$

where β is the optical thickness at 1μm and α explains the change of AOD with wavelength. β accounts for the amount (load) of aerosols in the atmosphere and α has to do with the size of the aerosols; the larger α, the smaller the particles, with maximum value of 4, corresponding to molecular scattering (Rayleigh scattering).
Cachorro et al (1989) proved that measurements could be well explained with this formula in the visible range and some authors have also shown its validation in the UV band (e.g. Meleti & Cappellani, 2000, Wenny et al, 2001).
We have chosen the wavelength of reference for AOD at 368 nm because this is the lowest λ considered by the sun photometer that measures AOD at De Bilt (Sun Photometer UV, Yes Inc.); also, 368 nm is a common wavelength used by sun photometers in the UV range.
We consider wavelength independent values of SSA and G as a first approximation because their spectral dependence is unknown (for SSA) and estimated to be small (for G). Reuder & Schwander found, by Mie-calculations, variations in SSA, from 280 to 400 nm, of about +3% for both low (AOD at 400 nm of 0.10 and continental maritime aerosols) and high (0.80 and continental polluted aerosols) pollution conditions. For G, the variations were of 1.2% and 2.7% for these two cases, respectively. It could be, for certain chemical compositions of aerosols that the wavelength dependence is larger, but spectrally resolved measurements of these parameters in the UV range are not available; usually, SSA and G measurements are obtained by inversion techniques from broad-band total or visible measurements (e.g. Hänel, 1994)

32 Results ←

We perform a sensitivity study in order to know the effects of the change of each aerosol parameter on UVI and decide which ones have to be included in the aerosol-effect parameterisation.
Aerosol optical depth at 368 (AOD_{368}), Ångström's α (alpha), single scattering albedo (SSA) and asymmetry factor (G), as these are the parameters considered in TUV model, take part in the sensitivity study. Table 32 shows the chosen reference values for these four parameters together with the variations considered for each one.

Table 32 Reference values and variations considered for the four aerosols parameters taking part in the sensitivity study.

Parameter	Reference	Variations considered
SSA	0.9	0.6, 0.65, 0.70, 0.75, 0.8, 0,85, 0,95, 1
G	0.7	0.5, 0.6, 0.8, 0.9
alpha	1.4	0, 0.4, 0.9, 1.9, 2.4, 2.9
AOD_{368}	0.3	0, 0.1, 0.2, 0.4, 0.5, 0.6, 0.7, 1.0, 1.2, 1.5

The reference values of AOD_{368} and alpha have been taken on basis of 4-years (1997-2000) AOD measurements in De Bilt (Stammes & Henzing, 2000) with the SPUV sun photometer; for this period the mean AOD_{368} and alpha values are 0.346 and 1.396, with standard deviations of 0.210 and 0.432, respectively. The reference values of SSA and G have been taken as typical values for UV, as stated by Madronich (1993) (see Chapter 1).
Tables 3a-d show values of SSA, G, alpha and AOD_{368} found in some studies. Some of the optical depths shown have been converted from other wavelengths through the Ångström's formula using mean alpha values reported by the authors. G and SSA values were retrieved from broadband quantities so they do not refer to any wavelength.
In Table 3a we see a wide range of SSA, from strong absorption aerosols (with SSA=0.35) in urban-industrialised conditions until almost complete scattering aerosols (with SSA=0.993). As shown in Table 2, we consider values of SSA from 0.6 to 1 for the sensitivity study, which covers most of the situations and may leave out some aerosols conditions that take place in very polluted urban regions, which, as stated in Chapter 2, are out of the coverage of the present work.
Values from 0.47 to 0.86 are shown in Table 3b for G. Mean values of G also covers a large range (0.47-0.77). We have chosen the interval 0.5 to 0.9 of G values for the sensitivity study, which takes into account almost all of these situations.
Wenny et al, (2001) reported alpha measurements from about 0.2 until almost 4 (see Table 3c); all the other measurements shown are within this interval. We have limited the range up to 2.9 (small aerosols). Larger values are quite unlikely and not included in our study.
Concerning the optical depths records, Table 3d shows values up to 2.68 (for Ispra). The averages are much lower, up to 0.58, also in Ispra. We take an upper limit of 1.5 because it contains all the 4-years measurements in De Bilt and the great majority of conditions that occur in non-extremely polluted sites.

We represent in figure 1 UVI calculated for the reference case and the case without aerosols (to make evident the effects of the reference aerosols on UVI) as a function of SZA, from 0 to 85 degrees, and TOZ, from 250 to 450 DU. These ranges are considered to evaluate the differences in UVI due to aerosols. The chosen range for TOZ covers the most common values (about 99% of the situations of De Bilt are in this range). For SZA, we do not consider 90 degrees because the UVI values are very small and the error of the calculations done with the two-streams code start to have important errors.
Figure 1 shows UVI values up to 14 for the reference case and up to 16 for the case without aerosols. There is a strong dependence on SZA and also a large effect of TOZ. Notice that a change in TOZ from 250 to 450 DU can lead UVI to be reduced to half its value (for low SZA).

In total, we have taken into account 28 cases for the sensitivity study (see Table 2). For each case, we have calculated the ratio and the absolute difference in UVI with respect to the reference case as a function of TOZ (from 250 to 450 DU with steps of 10 DU) and SZA (from 0 to 85 with steps of 5 degrees). All theses 56 graphics are collected in the Appendix, at the end of this report.
Table 4 shows the maximum relative and absolute differences found for each parameter and all the TOZ and SZA values. We see that, for the ranges selected, changing G or alpha has a relative effect (with respect to reference values) less than 3.5% and produces a variation in UVI of up to ±0.4. Much more effect is observed for SSA, with maximum relatives changes of −19% and 8% and absolute variations in UVI from −2.0 to 0.8. The AOD_{368}, as expected, produces the largest effect, with percentages ranging between −40 and 14% and absolute values, from −4.7 to 1.3.

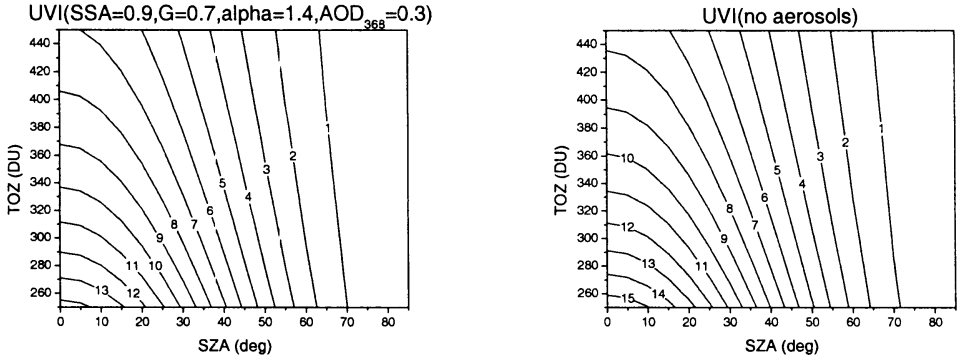

Figure 31 UVI as a function of TOZ and SZA for the reference case of the sensitivity study (left) and for no aerosols conditions (right).

Tables 33ad Values of SSA (a), G (b), alpha (c) and AOD_{368} (d) reported by several authors

a SSA

Period	Site	Mean	Min	Max	Reference
10 days	Melpitz	-	0.79	0.93	von Hoyningen-Huene *et al* (1996)
181 samples	4 German sites and 2 Italian	0.831	0.586	0.993	Hänel (1994)
1973-79	Urban-industrial regions in USA	-	0.35	0.77	Waggoner *et al* (1981)
1973-77	Urban-residencial regions in USA	-	0.65	0.93	Waggoner *et al* (1981)
1974-79	Remote regions in USA	-	0.86	0.97	Waggoner *et al* (1981)

b G

Period	Site	Mean	Min	Max	Reference
1 year	Maisach	0.47-0.63	-	-	von Hoyningen-Huene & Wendisch (1994)
1 year	Leipzig	0.53-0.69	-	-	von Hoyningen-Huene & Wendisch (1994)
181 samples	4 German sites and 2 Italian	0.77	0.72	0.86	Hänel (1994)

c alpha

Period	Site	Mean	Min	Max	Range (nm)	Reference
4 years	De Bilt	1.398	0.184	2.448	368-871	Stammes ()
6 months	Black Mountain	1.86	≈0.2	≈4	317-368	Wenny *et al*, (2001)
1 year	Ispra	1.26	0.64	2.15		Meleti & Capellani, 2000
1 year	Maisach	0.44-1.34	-	-	350-1100	von Hoyningen-Huene & Wendisch (1994)
1 year	Leipzig	0.60-1.08	-	-	350-1100	von Hoyningen-Huene & Wendisch (1994)
1 year	Zingst	0.42-1.17	-	-	350-1100	von Hoyningen-Huene & Wendisch (1994)

d AOD_{368}

Period	Site	Mean	Min	Max	Reference
4 years	De Bilt	0.346	0.012	1.230	Stammes ()
6 months	Black Mountain	0.330	0.030	1.199	Wenny *et al*, 2001
1 year	Ispra	0.592	0.028	2.682	Meleti & Capellani, 2000
1 year	Maisach	0.059-0.485	-	-	von Hoyningen-Huene & Wendisch (1994)
1 year	Leipzig	0.227-0.521	-	-	von Hoyningen-Huene & Wendisch (1994)
1 year	Zingst	0.115-0.449	-	-	von Hoyningen-Huene & Wendisch (1994)

In brackets the total range of absolute effects is given, which is an upper limit for the uncertainties due to the considered parameter.. While for G and alpha the maximum uncertainty is 0.8 and 0.7, respectively, for SSA it would be up to 2.8 and for AOD_{368}, up to 6.
No correspondence exists between the maximum relative and absolute values in Table 34. What can be said is that the relative values that correspond to the maximum absolute errors are lower that the ones reported in this table. For example, the maximum effect of -4.7 in UVI reported for AOD_{368} corresponds to a -33%, which is much lower than the -40% shown as the maximum relative value. The corresponding absolute value for this last percentage is -1.0.
Tables 35a-c collect, for each value considered for each parameter, the range of the relative values, the maximum absolute effect on UVI and the actual relative and absolute effects for 0, 30 and 60 degrees of SZA and 320 DU of TOZ (which is the mean value for De Bilt, with an standard deviation of 31 DU); all these values are calculated with respect to the reference conditions. We see that the range of relative variation for each value of SSA, G and AOD is almost completely explained by SZA. For alpha, TOZ plays a little bit more important role. AOD_{368} shows the maximum dependences in SZA from 0 to 60 degrees, up to 6% (for AOD_{368}=1.5). For SSA, the maximum SZA dependence is 4% (for SSA=0.6), while for G and alpha this is much smaller, 0.8% and 0.3%, respectively.
Notice also that for AOD_{368}, SSA and G the absolute variations are quite symmetric with respect to the reference values. For AOD_{368} and G this is also true for each of the three values of SZA.

We can summarise the results of the sensitivity study as follows:

- The effect of aerosols on UVI is almost independent of TOZ. In first but good approximation this allows us to treat the aerosol effect independent of TOZ.
- AOD_{368} has an important SZA dependence (up to 6% from 0 to 60 degrees). SSA has less remarkable dependence on SZA (up to 4%) and for G and alpha it is very weak.
- As expected, AOD_{368} is the most important parameter to explain the effect of aerosols on UVI, with a maximum absolute effect of 6 in UVI. However, it has been found that SSA plays also an important role, being able to induce a maximum absolute effect in UVI of 2.8.
- Variations in G and alpha are of much less importance, with maximum absolute effects on UVI of ±0.8.

This is consistent with the results that Reuder & Schwander (1999) reported. They found that about 80% of the total effect produced by aerosols on UVI could be explained only with the aerosol optical thickness (about 55%) and the single scattering albedo (about 25%).
Based on these results we decided to consider AOD_{368}, SSA and SZA in the parameterisation of the aerosols effects on UVI and fix G and alpha to the reference conditions. The way we derive the aerosol parameterisation is explained in Chapter 4.

Table 34 Maximum relative and absolute effects on UVI observed for the four parameters in the range considered. Values in brackets show the ranges of the relative and absolute effects.

Parameter	Range	Relative effect on UVI (%)	Absolute effect on UVI	
SSA	0.6-1	-19 / 7.6	-2.0 / 0.8	(2.8)
G	0.5-0.9	-3.2 / 3.5	-0.4 / 0.4	(0.8)
alpha	0-2.9	-3.2 / 2.4	-0.4 / 0.3	(0.7)
AOD_{368}	0-1.5	-40 / 14	-4.7 / 1.3	(6.0)

Tables 3a-d Relative ranges, maximum absolute effects and relative and absolute effects for 0, 30 and 60 degrees of SZA and 320 DU of TOZ for all the values of SSA (a), G (b), alpha (c) and AOD_{368} (d) considered.

a SSA		0.6	0.65	0.7	0.75	0.8	0.85	0.95	1
relative range (%)		-19/-13	-17/-11	-13/-9	-10/-7	-6.9/-4.8	-3.5/-2.5	2.6/3.7	5.2/7.6
max. abs. effect		-2.0	-1.7	-1.3	-1.1	-0.7	-0.4	0.4	0.8
0 deg	relative	-14%	-11%	-9.2%	-7.3%	-5.0%	-2.5%	2.6%	5.4%
	absolute	-1.4	-1.2	-1.0	-0.8	-0.5	-0.3	0.3	0.6
30 deg	relative	-15%	-13%	-10%	-7.9%	-5.4%	-2.7%	2.9%	5.9%
	absolute	-1.1	-0.9	-0.7	-0.6	-0.4	-0.2	0.2	0.4
60 deg	relative	-18%	-16%	-13%	-10%	-6.6%	-3.4%	3.5%	7.2%
	absolute	-0.3	-0.3	-0.2	-0.2	-0.1	-0.06	0.06	0.1

b G		0.5	0.6	0.8	0.9
relative range (%)		-3.2/-2.7	-1.7/-1.3	1.3/1.7	2.6/3.5
max. abs. effect		-0.4	-0.2	0.2	0.4
0 deg	relative	-2.7%	-1.4%	1.3%	2.7%
	absolute	-0.3	-0.1	0.1	0.3
30 deg	relative	-2.9%	-1.4%	1.4%	2.9%
	absolute	-0.2	-0.1	0.1	0.2
60 deg	relative	-3.2%	-1.7%	1.7%	3.5%
	absolute	-0.06	-0.03	0.03	0.06

c alpha		0	0.4	0.9	1.9	2.4	2.9
relative range (%)		1.1/2.4	0.8/1.8	0.4/0.9	-1.0/-0.4	-2.0/-0.9	-3.2/-1.4
max. abs. effect		0.3	0.2	0.1	-0.1	-0.3	-0.4
0 deg	relative	1.9%	1.4%	0.7%	-0.8%	-1.7%	-2.6%
	absolute	0.2	0.1	0.08	-0.08	-0.2	-0.3
30 deg	relative	2.0%	1.5%	0.8%	-0.8%	-1.8%	-2.8%
	absolute	0.1	0.1	0.06	-0.06	-0.1	-0.2
60 deg	relative	2.2%	1.6%	0.8%	-0.9%	-1.9%	-2.9%
	absolute	0.04	0.03	0.02	-0.02	-0.03	-0.05

d AOD_{368}		0	0.1	0.2	0.4	0.5	0.6	0.7	1.0
relative range (%)		8.7/14	5.9/9.1	3.0/4.5	-4.3/-2.9	-8.2/-5.9	-12/-9.7	-16/-12	-26/-20
max. abs. effect		1.3	0.9	0.4	-0.4	-0.9	-1.3	-1.7	-2.9
0 deg	relative	9.0%	6.1%	3.0%	3.0%	-6.0%	-8.9%	-12%	-20%
	absolute	1.0	0.6	0.3	-0.3	-0.6	-0.9	-1.3	-2.1
30 deg	relative	10%	6.8%	3.4%	-3.3%	-6.6	-10%	-13%	-22%
	absolute	0.7	0.5	0.2	-0.2	-0.5	-0.7	-0.9	-1.6
60 deg	relative	14%	8.9%	4.3%	-4.1%	-8.0%	-12%	-15%	-25%
	absolute	0.3	0.2	0.08	-0.08	-0.1	-0.2	-0.3	-0.5

		1.2	1.5
relative range (%)		-32/-25	-40/-32
max. abs. effect		-3.7	-4.7
0 deg	relative	-25%	-33%
	absolute	-2.7	-3.5
30 deg	relative	-27%	-35%
	absolute	-2.0	-2.5
60 deg	relative	-31%	-39%
	absolute	-0.6	-0.7

4 Aerosols Effect Parameterisation

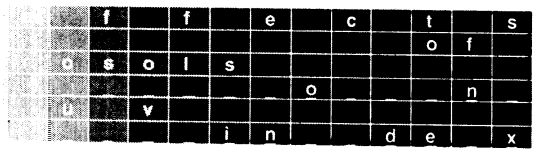

In Chapter 3 we have seen that AOD_{368} and SSA can induce differences in UVI up to 6 and 2.8, respectively, while alpha and G affect UVI less than 0.8. We have also seen important dependences of the effect of AOD_{368} and SSA on SZA. Because of these results we have decided to develop a parameterisation that explains the effects of aerosols on UVI considering SZA, AOD_{368} and SSA as parameters. As stated in section 3.1, estimations of SSA are rarely available (especially in the UV range) but climatic values could be taken as a function of different air mass types and origins for each site as, for example, von Hoyningen-Huene & Wendisch (1994) did.

Here we derive a parameterisation based on the TUV model that explains the aerosol relative effect on UVI. We have divided the process in two steps; first consider only the effects of SZA and AOD368 (fixing SSA at the reference value of 0.9) (4.1) and then add the contribution of this parameter (4.2). At the end of this Chapter we discuss the errors of the parameterisation (4.3) with respect to TUV calculations.

4.1 AOD and SZA Effects ←

To parameterise the effects of AOD_{368} and SZA we have made some calculations of UVI with the TUV model. Table 4.1 shows the conditions considered. The ranges are almost the same as the ones taken for the sensitivity study in Chapter 3. In this case, we only reach 80 degrees in SZA because it is enough for practical applications. We consider a larger density of values of SZA from 60 to 80 degrees because this has appeared convenient, as discussed below.

Although we have seen in Chapter 3 that aerosol and ozone effects can be almost completely separated, we also have considered different values of TOZ (from 250 to 450 DU), to make this fact more evident. SSA, G and alpha are set as the reference values considered for the sensitivity study. All the other modelling conditions are set as explained in Table 3.1.

Table 4.1 Modelling conditions considered for UVI calculations with TUV

Parameter	Values considered
AOD_{368}	from 0 to 1.5 with 0.5 steps
SZA	0, 15, 30, 45, 60, 65, 70, 75, 80 degrees
TOZ	250, 300, 350, 400, 450 DU
SSA	0.9 constant
G	0.7 constant
alpha	1.4 constant

The magnitude to be parameterised is the ratio

$$\frac{UVI(SZA,TOZ,AOD_{368})}{UVI(SZA,TOZ,0,)} \qquad (4.1)$$

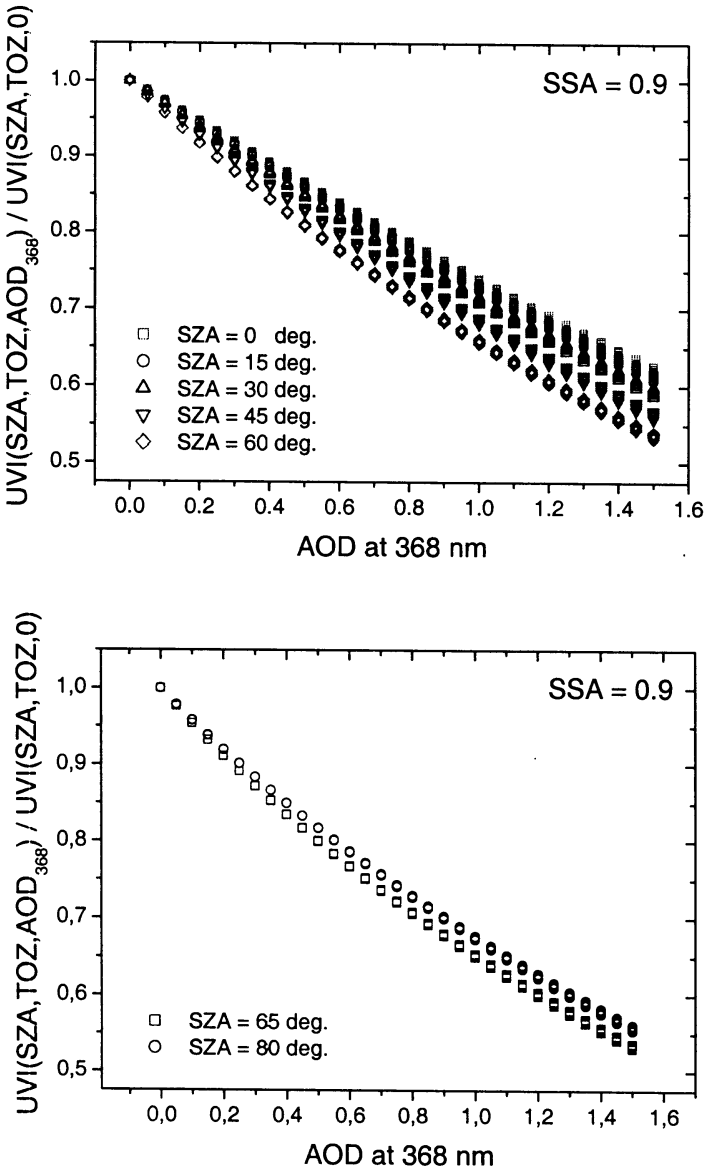

Figure 41 Representation of the relative aerosol effect (from TUV calculations) as a function of AOD_{368} and for 0, 15, 30, 45, 60 (up), 65 and 80 (down) degrees of SZA. Points corresponding to TOZ=250, 300, 350, 400 and 450 DU are also represented for each value of SZA.

which explains the relative effect of aerosols on UVI. Figure 41 shows its representation as a function of AOD_{368}, SZA and TOZ. We have used two representations to avoid the superposition of the points; plots for 70 and 75 degrees are not shown for the same reason. The superposition takes place since, as already seen in Chapter 3, the maximum aerosol effect is found near 65 degrees and, from this angle on, the aerosol effect diminishes. This is because as SZA increases the direct component, which aerosols attenuate, looses influence in favour of the diffuse, which is increased by aerosols.

Notice that the points corresponding to TOZ variation for each SZA are almost superimposed, most of all for low values of AOD_{368}. This gives clear evidence that the aerosol and ozone effects can be studied separately with very small errors.

We see that the dependence on AOD_{368} is quite linear (as also pointed out in Chapter 3). This becomes less true for large values of AOD_{368} and SZA. Because of this, in order to get the best fit, we have tried an exponential decrease function to explain the combined SZA and AOD_{368} effects with one independent parameter b, such as

$$\frac{UVI(SZA,TOZ,AOD_{368})}{UVI(SZA,TOZ,0,)} = e^{-b(SZA,SSA=0.9)AOD_{368}} \qquad (42)$$

where b is considered to depend on SZA and SSA (now fixed at 0.9). Trying this kind of fit, we get the results collected in Table 42. The value of b ranges between 0.3 and 0.4 and the fits always have regression coefficients greater than 0.997, showing a good degree of agreement. Figure 42 shows its representation as a function of the cosine of SZA. We have detected that for low values of SZA (large values of cos(SZA)) b has a perfect linear dependence (with a regression coefficient of 0.99999 between 0 and 45 degrees), showing a clear cosine dependence of the aerosol effect ruled mostly by the direct component. When reaching 65-70 degrees the maximum aerosol effect on UVI is achieved and for larger angles this effect diminishes, as commented above, due to the diffuse component influence. We needed more resolution for large SZA in order to be able to completely explain this evolution.

Figure 42 also shows the 3rd order polynomial curve we have considered to fit the points. The expression is:

$$b = 0.30 + 0.74\mu_0 - 1.27\mu_0^2 + 0.54\mu_0^3 \qquad (43)$$

where $\mu_0 \equiv \cos(SZA)$. The regression coefficient for this fit is 0.993.

Table 41 Values of b, they error and the regression coefficients found using the fitting formula 42 for each value of SZA and for SSA=0.9

SZA	b	errb	r^2
0	0.3092	0.0008	0.9975
15	0.3171	0.0007	0.9978
30	0.3404	0.0006	0.9986
45	0.3781	0.0004	0.9994
60	0.4185	0.0004	0.9997
65	0.4284	0.0008	0.9984
70	0.428	0.001	0.9975
75	0.4151	0.0007	0.9990
80	0.3938	0.0005	0.9993

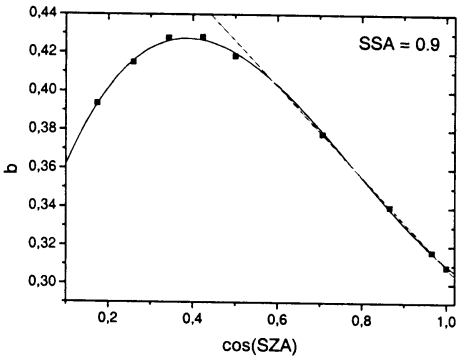

Figure 42 Representation of the values of b (reported in table 42) as a function of the cosine of SZA. A polynomial fit of all the points (black line) and linear fit for SZA<45 (gray line) are also shown

42 SSA Effect ←

To explain the SSA effect we have performed the same calculations described in Table 41 for four values selected between 0.6 and 1.0 (which is the range considered in the sensitivity study, Chapter 3): 0.6, 0.75, 0.8, and 0.98. There is not a special reason for these values; they are just the ones used in previous tests that we made.

Figure 43 shows the representations of the relative effect for these four values and only SZA between 0 and 60 (to avoid superpositions). Remarkable is the great difference between the extreme values of SSA. For SSA=0.6 the curves are non linear and the effect on UVI reaches about 80% (for SZA=60 degrees and AOD_{368}=1.5). For SSA=0.98 the representation is linear for all values of SZA and the maximum aerosol effect is about 30%. This gives clear evidence of the necessity to include SSA in the parameterisation.

For each value of SSA, we have made the fits explained by expression 42. The values of b found for each SSA and SZA are collected in Table 42. We see that b ranges between 0.16 and 1.1. Notice that we get better fits for low SSA (with almost

all r^2 larger than 0.999); for SSA=0.98 the points are less well fitted with an exponential function because they are linear.

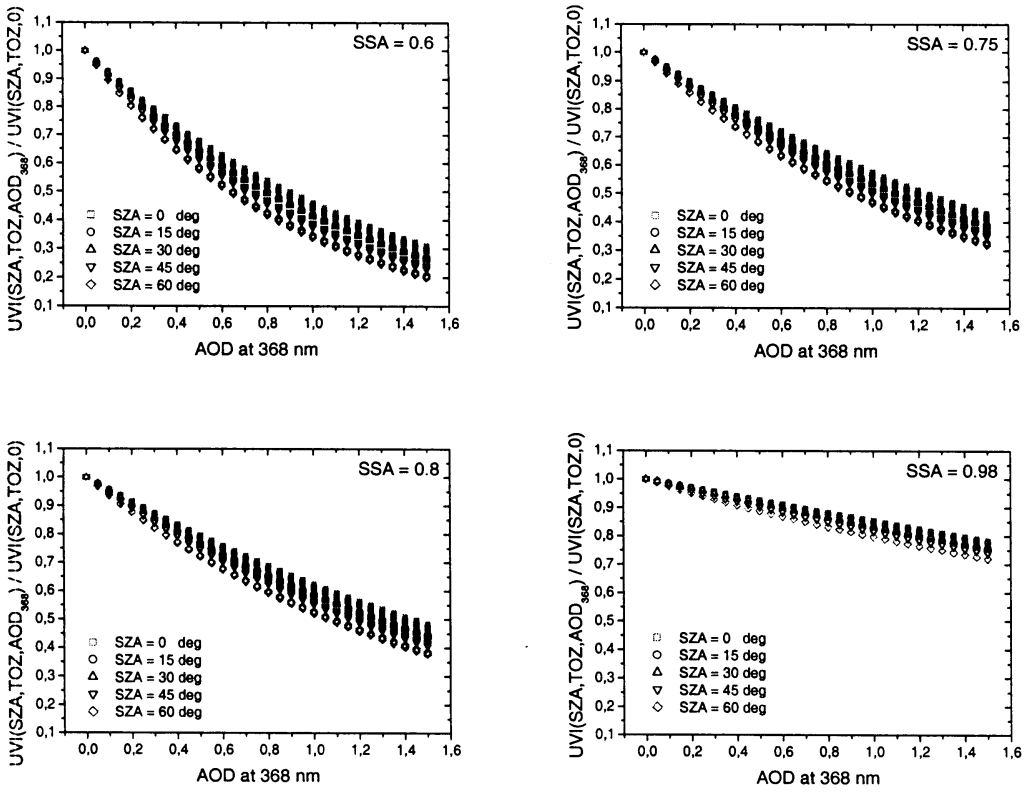

Figure 43 Representation of the aerosol relative effect (from TUV calculations) as a function of AOD_{368}, for SZA between 0 and 60 degrees and TOZ between 250 to 450 DU. Representations are made for four values of SSA: 0.6, 0.75, 0.8 and 0.98.

Table 42 Values of b, they error and the regression coefficients found using the fitting formula 42 for each value of SZA and for SSA=0.6, 0.75, 0.8 and 0.98

SSA = 0.6				SSA = 0.75			
SZA	b	errb	r^2	SZA	b	errb	r^2
0	0.788	0.001	0.9995	0	0.560	0.001	0.9988
15	0.808	0.001	0.9994	15	0.574	0.001	0.9989
30	0.866	0.001	0.9995	30	0.6144	0.0009	0.9991
45	0.963	0.001	0.9996	45	0.6810	0.0008	0.9995
60	1.072	0.001	0.9996	60	0.7543	0.0007	0.9997
65	1.094	0.001	0.9995	65	0.7684	0.0009	0.9996
70	1.096	0.002	0.9992	70	0.769	0.001	0.9993
75	1.070	0.002	0.9989	75	0.751	0.001	0.9991
80	1.018	0.002	0.9991	80	0.714	0.001	0.9994

SSA = 0.8				SSA = 0.98			
SZA	b	errb	r^2	SZA	b	errb	r^2
0	0.480	0.001	0.9984	0	0.1596	0.0003	0.9979
15	0.492	0.001	0.9986	15	0.1645	0.0003	0.9984
30	0.5263	0.0009	0.9989	30	0.1788	0.0002	0.9994
45	0.5830	0.0007	0.9994	45	0.2017	0.0002	0.9997
60	0.6450	0.0006	0.9997	60	0.2259	0.0005	0.9976
65	0.654	0.001	0.9991	65	0.2348	0.0009	0.9919
70	0.654	0.001	0.9986	70	0.234	0.001	0.9895
75	0.641	0.001	0.9991	75	0.2235	0.0007	0.9946
80	0.6099	0.0008	0.9994	80	0.2103	0.0005	0.9966

Figure 44 shows the representation of the relative values of b, with reference to the value of 0 degrees SZA, as a function of the cosine of SZA for SSA=0.6, 0.75, 0.8, 0.9 and 0.98. A very similar pattern is seen, always with the maximum aerosol effect between 65 and 70 degrees. For low SZA the points are almost superimposed, while for large SZA some vertical differences appear without a clear pattern.

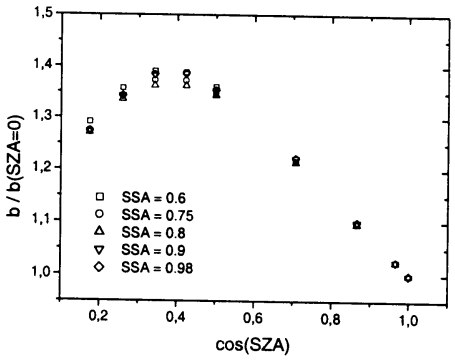

Figure 44 Representation of the relatives values of b, with respect to their values at 0 degrees of SZA as a function of the cosine of SZA for SSA=0.6, 0.75, 0.8, 0.9 and 0.98

Table 43 shows the ratio between b for each value of SSA and b for the reference value (SSA=0.9) for all SZA. We see ratios from about 0.5 (for SSA=0.98) to about 2.5 (for SSA=0.6). The maximum variations of these ratios as a function of SZA are 1.6%, 1.1%, 1.6% and 6.2% for 0.6, 0.75, 0.8 and 0.98 of SSA, respectively. The former case gives a much larger relative dependence. The absolute maximum dependence on SZA gives more similar values: 0.041, 0.019, 0.025 and 0.032, respectively.

As a first approximation, we can consider that no dependence on SZA exists and take a representative value of the ratio b/b(SSA=0.9) for each value of SSA. These representative values have been found doing the average of the ratios from 0 to 65 degrees. We don't consider the larger values of SZA in order to be able to describe better the lower angles, which are of more practical interest (because they have a larger UVI associated).

Figure 45 shows the representation of these mean ratios as a function of SSA. Notice that the representation of the points is very linear, which allows us to explain them through a line. To fit the points we have imposed that for SSA=0.9 the ratio is 1. The regression coefficient obtained is 0.9984 with a slope of 5.26 ± 0.08.

Table 43 Ratios between b for each value of SSA and b for SS=0.9 for all SZA values

	SSA			
SZA	0.6	0.75	0.8	0.98
0	2.549	1.811	1.552	0.5162
15	2.548	1.810	1.552	0.5188
30	2.544	1.805	1.546	0.5253
45	2.547	1.801	1.542	0.5335
60	2.562	1.802	1.541	0.5398
65	2.554	1.794	1.527	0.5481
70	2.561	1.797	1.528	0.5467
75	2.578	1.809	1.544	0.5384
80	2.585	1.813	1.549	0.5340

So, we have already found an expression of b as a function of SZA and SSA:

$$b(SZA, SSA) = (0.30 + 0.74\mu_0 - 1.27\mu_0^2 + 0.54\mu_0^3) \cdot (1 - 5.26(SSA - 0.9)) \qquad (44)$$

which, put in the expression 42, gives the proposed parameterisation of the relative effect of aerosols on UVI.

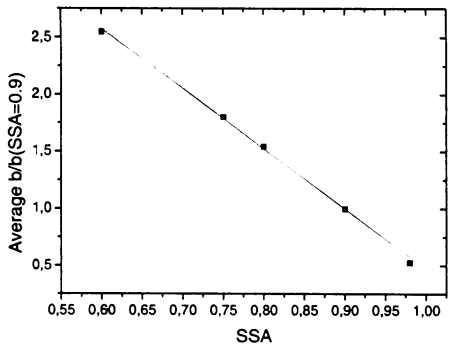

Figure 45 Representation of the average values found for the ratio b/b(SSA=0.9) as a function of SSA. The linear fit of the points is shown in gray.

43 Error Analysis ←

To have an estimation of the errors of the aerosol parameterisation for a variety of conditions we base on the same calculations used to retrieve the parameterisation. Table 44 collects the maximum relative and absolute errors found for all conditions of SZA, TOZ, AOD_{368} and SSA. All relative errors are within ±3% while the absolute errors are at maximum ±0.2. Notice that the maximum absolute and relative negative errors are found for SSA=0.98, as a consequence of the worst fits obtained for this case, as commented in point 42.

Table 44 Maximum relative and absolute theoretical (compared with TUV calculations used for the retrieval) errors of the aerosol parameterisation

SSA	Max relative error	Max absolute error
0.6	-1.4 : 1.3%	-0.06: 0.04
0.75	-0.8 : 2.0%	-0.05: 0.12
0.8	-0.8 : 2.2%	-0.05: 0.15
0.9	-1.0 : 1.5%	-0.08: 0.13
0.98	-2.9 : 0.5%	-0.20: 0.00

Figure 46 collects the relative and absolute errors for all the conditions considered as a function of UVI, SZA, TOZ, AOD_{368} and SSA. It is seen that maximum absolute errors correspond to low SZA and TOZ and large values of UVI and AOD_{368}. In SSA we find much smaller absolute errors for SSA=0.6 than for SSA=0.98.

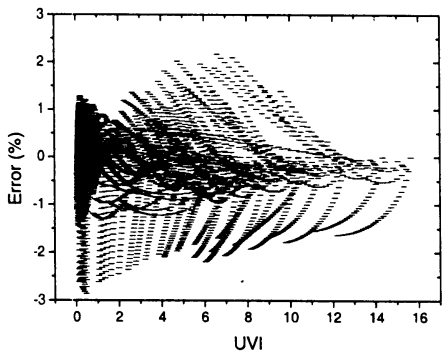

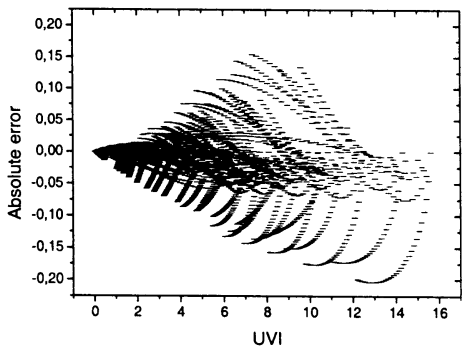

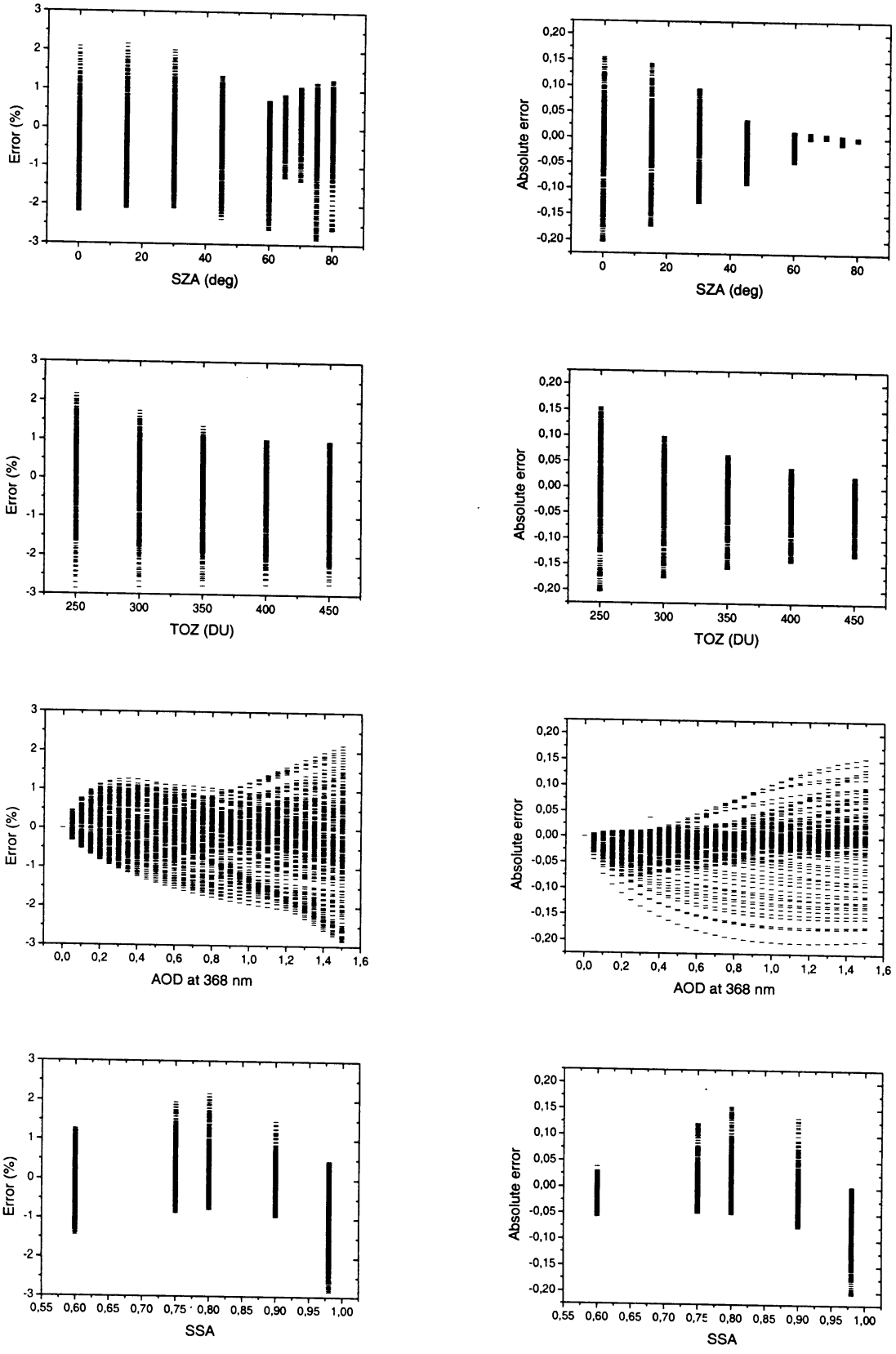

Figure 46 Relative and absolute errors of the TUV-based aerosol parameterisation as a function of UVI, SZA, TOZ, AOD_{368} and SSA

Maximum relative errors also correspond to large values of AOD_{368}. For SZA and TOZ no clear dependence of the relative errors is observed. The largest errors are found for medium and low values of UVI. In SSA, apart from 0.98, the distribution of the relative errors is similar for all the values.

5 UVI Algorithms

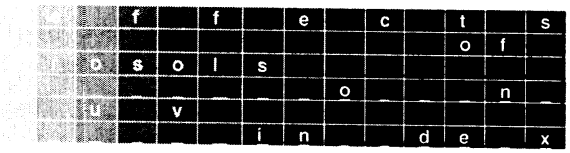

In Chapter 4 we have proposed a parameterisation to explain the relative effect of aerosols on UVI. However, an algorithm for UVI absolute calculations is needed for practical purposes. In this Chapter we propose a way to derive UVI as a function of SZA, TOZ and aerosol optical properties.
First, we present the empirical algorithm that is currently used for worldwide UVI forecasts by the GOME Fast Delivery Service (as mentioned in Chapter 1) (51) and, inspired on this we derive an algorithm based only on TUV model calculations that includes the aerosol effect parameterisation (52). At the end of the Chapter, a first test to validate this last algorithm is done with measurements taken in De Bilt (53).

51 Empirical Algorithm ←

As commented in Chapter 1, Allaart et al (2002) derived an empirical algorithm (hereon called UVI_{fun}) to perform fast UVI calculations and to be used for prediction purposes. GOME Fast Delivery Service currently uses UVI_{fun} for daily worldwide UVI forecasts (www.knmi.nl/gome_fd). Half a year (April-September 2000) of Brewer MKIII UVI and TOZ measurements in De Bilt and one year (1999) of the same kind of measurements in Paramaribo (Suriname) were used to derive this algorithm. UVI_{fun} considers two principal parameters: SZA and TOZ. It does not consider aerosols explicitly but in a hidden way since aerosols affected the measurements fitted. UVI_{fun} has the following expression:

$$UVI_{fun} = \left[E_0 \cdot S \cdot \mu_x \cdot \exp(-\frac{\tau}{\mu_x}) \right] \cdot \left[F \cdot X^G + \frac{H}{TOZ} + J \right] \qquad (51)$$

where E_0 is the Sun-Earth distance correction factor and

$$\mu_x = \mu_0 \cdot (1-\varepsilon) + \varepsilon \qquad X = 1000 \cdot \mu_0 / TOZ$$
$$\mu_0 = \cos(SZA) \qquad F = 2.0$$
$$\varepsilon = 0.17 \qquad G = 1.62$$
$$S = 1.24 Wm^{-2} nm^{-1} \qquad H = 280.0$$
$$\tau = 0.58 \qquad J = 1.4.$$

TOZ is expressed in DU.
Figure 51 shows UVI calculated with this algorithm as a function of SZA (from 0 to 85 degrees) and TOZ (from 250 to 450 DU) together with the same representation for UVI calculations made with the TUV model (UVI_{tuv}) for the reference case

considered in the sensitivity study in Chapter 3 (i.e. AOD_{368}=0.3, SSA=0.9, alpha=1.4, G=0.7). Notice that the two representations are quite similar. We present in Figure 52 the representations of the ratio and the difference between UVI_{fun} and UVI_{tuv}. We see relative differences between +4% and -27% and absolute deviations between -0.61 and 0.54. Maximum relative differences are observed for large values of SZA. This is not surprising because UVI_{fun} considers the Brewer MKIII angular response while UVI_{tuv} takes into account an ideal response. The absolute deviations for this range are very small. For low values of SZA we see an important difference between the TOZ dependence considered by UVI_{fun} and UVI_{tuv} with absolute deviations for whole TOZ range from about -0.6 to +0.5.

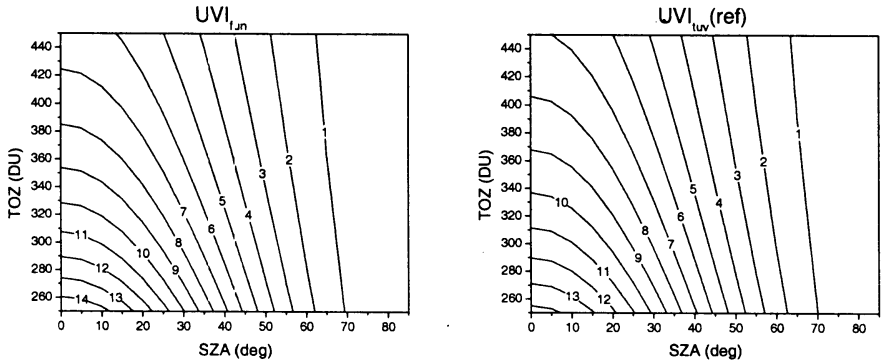

Figure 51 Representations of UVI_{fun} and UVI_{tuv} (for reference conditions) as a function of SZA and TOZ.

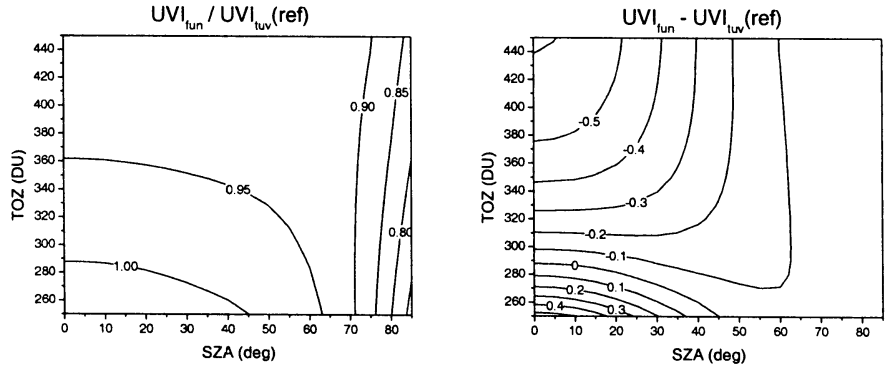

Figure 52 Representations of the ratio and the difference between UVI_{fun} and UVI_{tuv} (for reference conditions) as a function of SZA and TOZ.

Despite the differences observed, as they are intrinsic properties of both models, we can assume as a good approximation that the mean aerosol properties hidden in UVI_{fun} are similar in behaviour to the reference values considered in UVI_{tuv}. So we could use the aerosol parameterisation of Chapter 4 both to remove this aerosol effect (dividing UVI_{fun} by the expression 42) and include it again (multiplying) with the actual aerosol information so that UVI_{fun} considers aerosols explicitly. We will not do this here to avoid mixing empirical and theoretic information in a parameterisation, which could lead to difficult interpretations and also errors.
Because of this in the next section (52) we present an algorithm that we have derived insped by UVI_{fun} that does consider the aerosol parameterisation.

5.2 Theoretic Algorithm ←

A TUV-based algorithm to calculate UVI as a function of SZA, TOZ, AOD368, SSA and E0 (hereafter called UVI_{fituv}) is proposed here. We have derived it using the same expression as for UVI_{fun} (expression 5.1). The UVI calculations with TUV are done for non-aerosols conditions because the aerosol effect is already explained by the expression 4.2. The parameters considered in expression 5.1 have been found to have the following values in our fit:

$$\varepsilon = 0.18 \qquad F = 2.79$$
$$S = 1.22 Wm^{-2}nm^{-1} \qquad G = 1.41$$
$$\tau = 0.54 \qquad H = 280.0$$
$$J = 1.29.$$

where we have imposed H to take the same value as for UVI_{fun} in order to make the comparison more easy. We notice slightly different values as expected for the differences detected above between TUV calculations and UVI_{fun}.
UVI_{fituv} is completed by multiplication with expression 4.2 to consider the aerosol effects.
To theoretically validate UVI_{fituv} we have used the same TUV calculations described in Chapter 4. For SZA from 0 to 80 degrees, TOZ from 250 to 450 DU, AOD_{368} from 0 to 1.5 and SSA from 0.6 to 0.98 maximum relative errors of -8% and +6% and absolute errors of ±0.4 are found.
Figure 5.3 shows the relative and absolute errors for all the cases considered as a function of UVI_{tuv}, SZA, TOZ, AOD_{368} and SSA.
Relative errors have almost no dependence on SZA, TOZ, AOD_{368} and SSA. However, we see the maximum relative errors for values of UVI less than 7. The errors are much smaller for larger UVI values. The maximum absolute errors are concentrated around 7-8 in UVI and decrease for lower and larger values. For low SZA maximum absolute errors are reached and they are smaller than ±0.3 for SZA>30 degrees. For TOZ=250 DU, the maximum positive absolute errors are reached; for the rest of the TOZ values, the absolute errors show a similar range (between -0.35 and 0.15). A little bit larger errors are found for large values of AOD_{368} than small values. In SSA a smaller range of absolute errors is found for small values (0.6).
This results show that UVI_{fituv} has good agreement with TUV in a wide range of conditions.

5.3 First Validation with Measurements ←

We know that UVI_{fituv} gives good results in theory but comparisons with measurements are needed to test its practical utility.
Here we present a first comparison made with 4 years (1997-2000) of UVI, TOZ and AOD_{368} measurements in De Bilt. UVI and TOZ measurements are supplied by Brewer MKIII spectrophotometer and aerosol data is from the SPUV sun photometer. Daily mean TOZ values are considered. At maximum two values of AOD_{368} are available per day (morning and afternoon). These values are derived

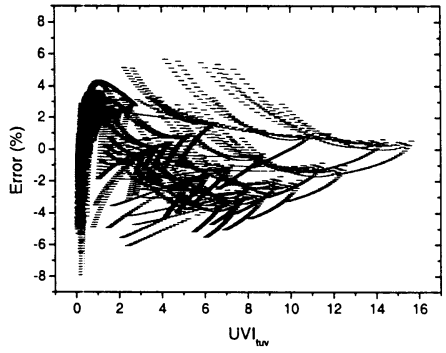
Error (%)
8
6
4
2
0
-2
-4
-6
-8
0 2 4 6 8 10 12 14 16
UVI$_{tuv}$

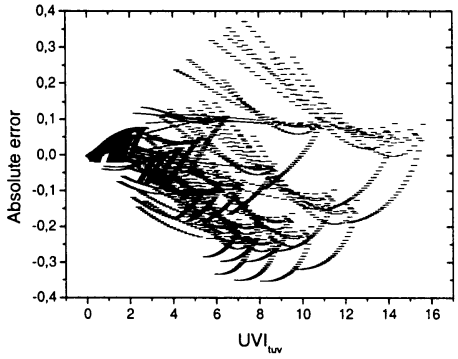
Absolute error
0,4
0,3
0,2
0,1
0,0
-0,1
-0,2
-0,3
-0,4
0 2 4 6 8 10 12 14 16
UVI$_{tuv}$

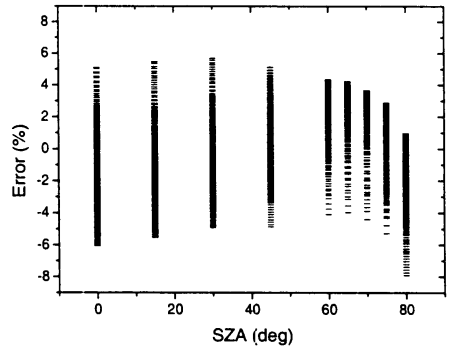
Error (%)
8
6
4
2
0
-2
-4
-6
-8
0 20 40 60 80
SZA (deg)

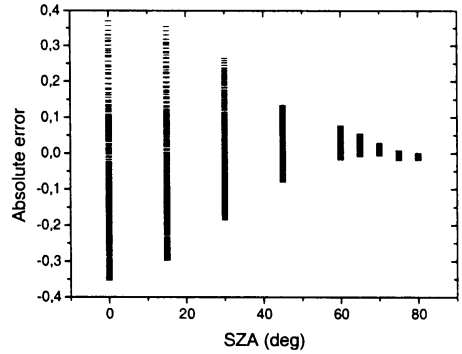
Absolute error
0,4
0,3
0,2
0,1
0,0
-0,1
-0,2
-0,3
-0,4
0 20 40 60 80
SZA (deg)

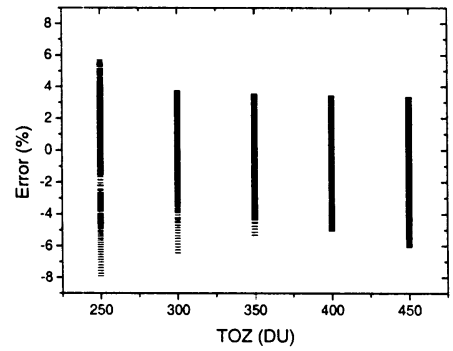
Error (%)
8
6
4
2
0
-2
-4
-6
-8
250 300 350 400 450
TOZ (DU)

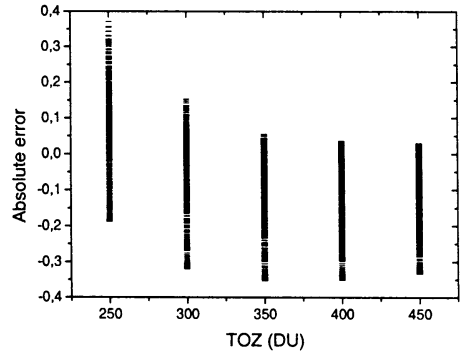
Absolute error
0,4
0,3
0,2
0,1
0,0
-0,1
-0,2
-0,3
-0,4
250 300 350 400 450
TOZ (DU)

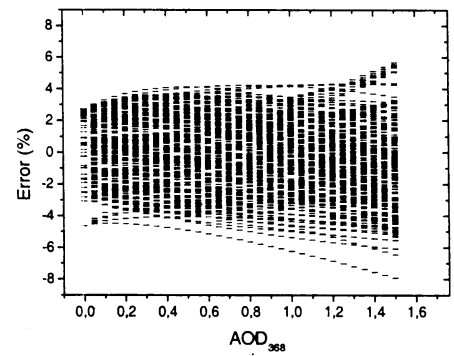
Error (%)
8
6
4
2
0
-2
-4
-6
-8
0,0 0,2 0,4 0,6 0,8 1,0 1,2 1,4 1,6
AOD$_{368}$

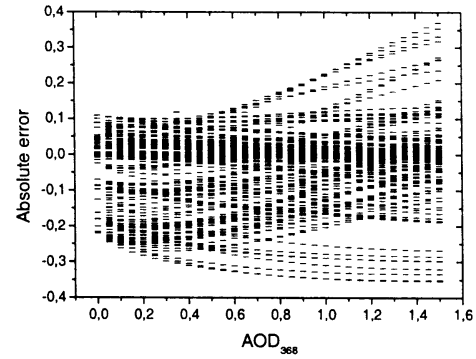
Absolute error
0,4
0,3
0,2
0,1
0,0
-0,1
-0,2
-0,3
-0,4
0,0 0,2 0,4 0,6 0,8 1,0 1,2 1,4 1,6
AOD$_{368}$

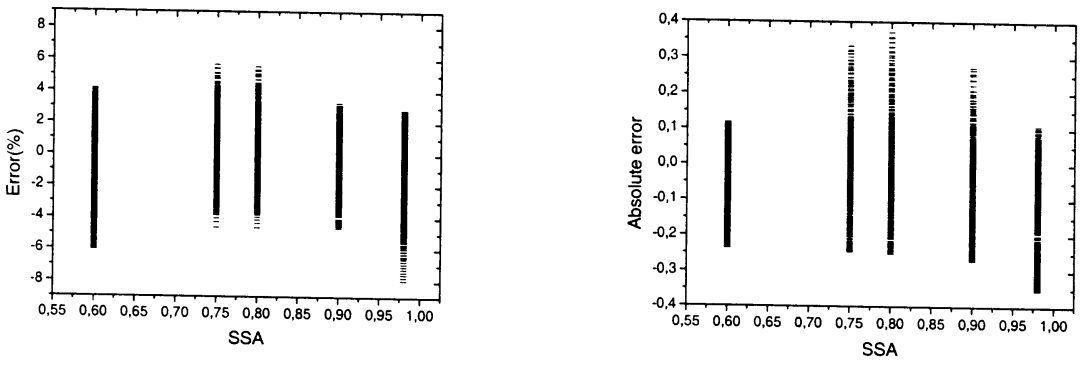

Figure 53 Relative and absolute errors of UVI_{fituv} as a function UVI_{tuv}, SZA, TOZ, AOD_{368} and SSA

using Langley plots that considers measurements with air masses from 2 to 6 (about 60 to 80 degrees of SZA) which restricts the period of measurements to early morning and late afternoon. However, we have supposed that the AOD_{368} is valid during the whole morning and the whole afternoon, respectively.

A filter to leave out the cloud situations was applied, resulting in 1460 records considered for the comparison. Figure 54 shows the histogram of the values of UVI, TOZ and AOD_{368}. The mean values are 1.6 (with a standard deviation of 1.8), 320 DU (31 DU), and 0.35 (0.21), respectively. Most of UVI values considered are very small because most of clear sky situations in De Bilt take place in the beginning of the morning and, as the day passes, the presence of clouds becomes more frequent.

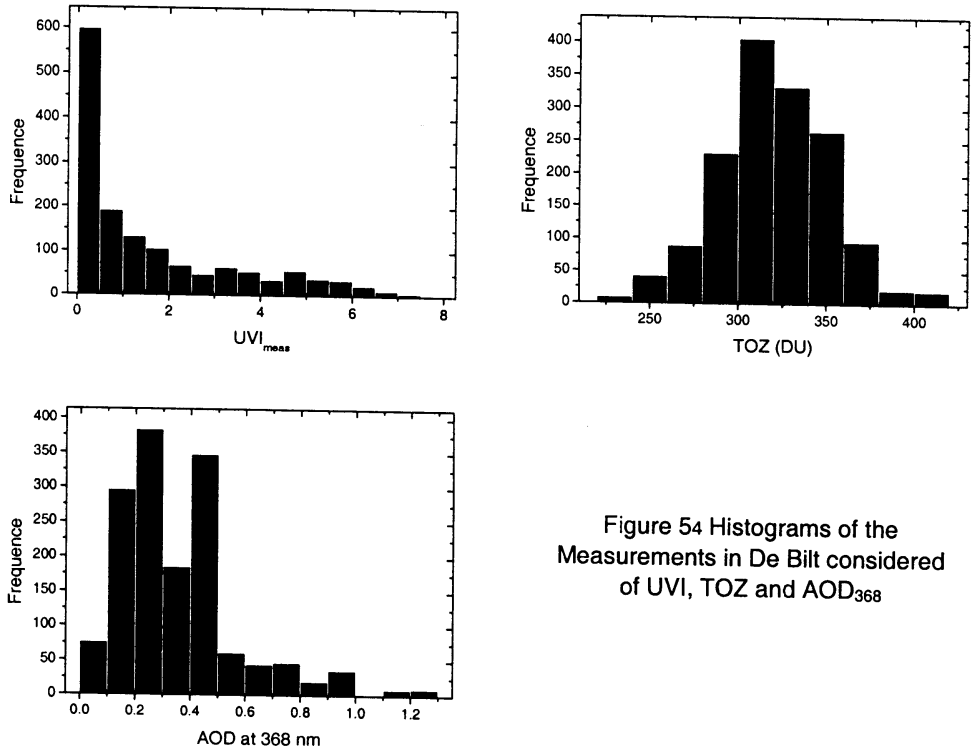

Figure 54 Histograms of the Measurements in De Bilt considered of UVI, TOZ and AOD_{368}

For the comparison with measurements, we have set SSA at the reference value because it is a typical value and we don't have more information about its value.

Figure 55 shows the representation model vs. measurement for the UVI_{fun} and UVI_{fituv} algorithms presented above. In gray, the linear fit is shown; the black line represents perfect agreement. At first sight the two representations show similar results with most points close to the black line.
Table 51 collects the numerical results of the fits. These numbers show that for both models a very good agreement with measurements is found. As already seen, the results are very similar, with the same regression coefficients, almost the same standard deviations (SD) and B a little bit larger for UVI_{fituv}.

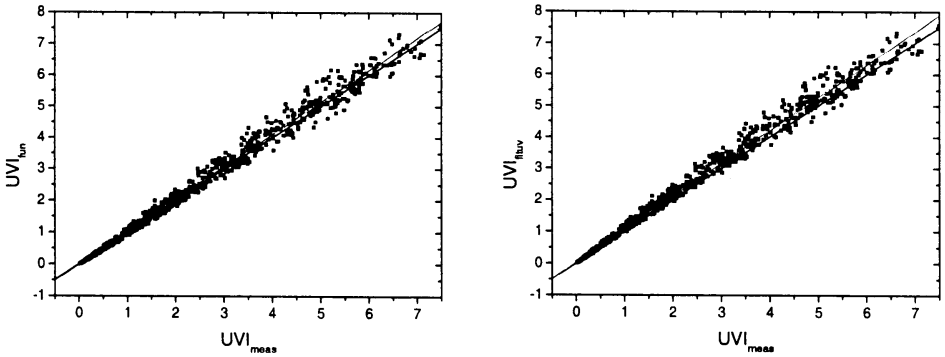

Figure 55 Model VS measurement for UVI_{fun} and UVI_{fituv} algorithms. Black line represents the perfect agreement (slope=1) and the gray line shows the linear fit of the points

Table 51 Estadistical Results of the linear fit of the points of the figure 55

Model	r^2	SD	Mean UVI	A	B
UVIfun	0.997	0.157	1.757	-0.011	1.028
UVIfituv	0.997	0.159	1.818	0.025	1.047

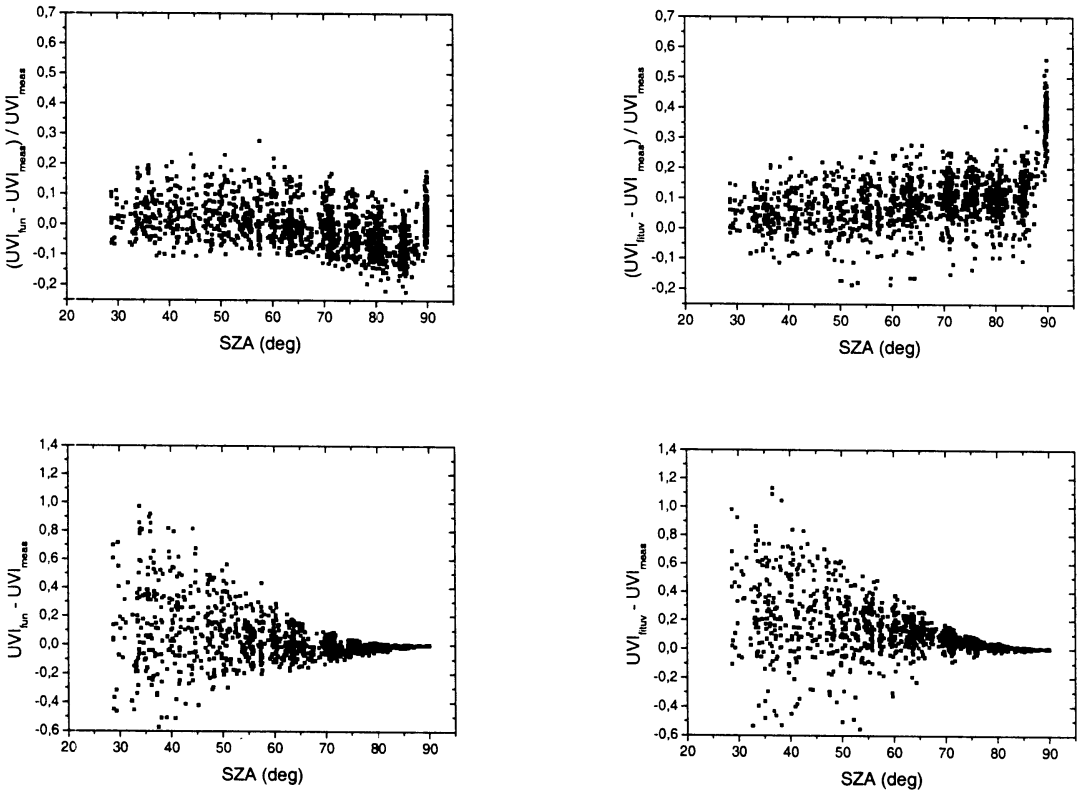

Figure 56 Representation of the relative and absolute errors of UVI_{fun} and UVI_{fituv} as a function of SZA

Figure 56 shows the representation of the relative and absolute errors as a function of SZA. For UVI_{fun} and UVI_{fituv} most of relative errors range within ±20%. Absolute errors are found from -0.6 to 1 for UVI_{fun} and up to 1.2 for UVI_{fituv}. Notice that for all the measurements SZA>30 degrees (and the mean SZA is 65 degrees); as seen above, maximum errors of UVI_{fituv} of ±0.3 would be expected and not the wider range observed here.
Again, the representations look quite similar, with a little bit less good results (more dispersed points) for UVI_{fituv}. Despite this algorithm has been retrieved only with SZA up to 80, we see that relative errors maintain in the same range until angles very close to 90 degrees. There, larger relative errors are found because UVI_{fittuv} considers an ideal angular response. From this, it can be stated that the Brewer MKIII angular response is sufficiently good up to angles very close to 90 degrees.
In Figure 57 we represent the absolute errors as a function of AOD_{368}. We see, as expected, that UVI_{fun} overestimates UVI for large values of AOD_{368}. However, for low optical depths both overestimations and underestimations are observed without a clear pattern. Notice that around AOD_{368}=0.3 the best agreement is found between UVI_{fun} and the measurements, which is consistent with our statement that this value of AOD_{368} is a good guess for the aerosols properties hidden in this algorithm.
For UVI_{fituv} underestimations of UVI are seen for large values of AOD_{368} and overestimations are detected for low values. The interval of best agreement is the same as for UVI_{fun}.

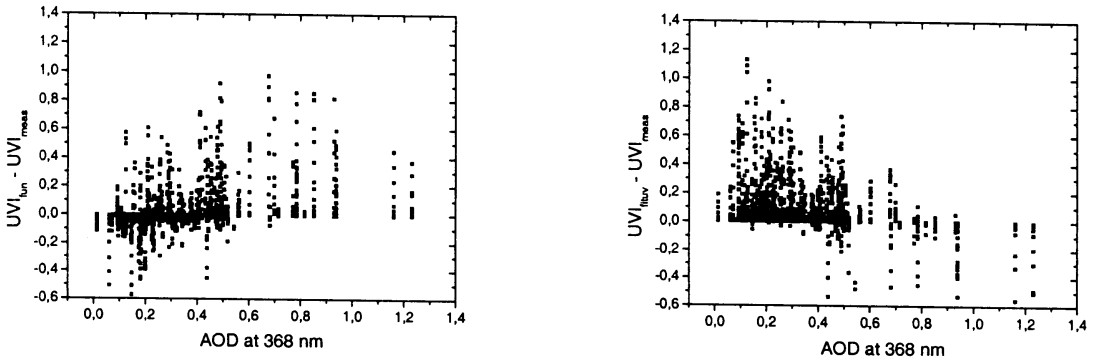

Figure 57 Representation of the absolute errors for UVI_{fun} and UVI_{fituv} as a function of AOD_{368}

All this results together make it not possible to state that the use of UVI_{fituv} to explain the results is better than the use of UVI_{fun}. From this comparison considered, we only can say that the two models give equivalent results. This already means implicitly that TUV calculations agree quite well with the Brewer measurements. However, the extra information about aerosols considered by UVIfituv seems not to have much beneficial effect. With AOD_{368} constant at the mean value (0.35) we have obtained very similar linear fits and behaviors than with inclusion of the measured AOD_{368} Figures 55-7.
We also have tried different values of SSA. For values of SSA larger than 0.9 the best linear fit is found and the relative errors are concentrated in a narrower band of values although UVI_{fituv} overestimates the measurements more. For lower values of SSA the linear gets worst.
As we believe, on basis of the analysis presented in point 52, that UVI_{fituv} should give better results than these observed, we suspect that the dataset used is not as

good as is needed to validate this algorithm. The fact that AOD_{368} is retrieved only considering very narrow periods of time could lead to important errors when extrapolating these measurements to the rest of the morning or afternoon. Also, UVI values are mostly very small, with an average SZA of 65 degrees. However, deeper analyses are needed to fully understand the results.

Apart from this, to perform a good validation, first of all, we would need a wider range of conditions with good accuracy and concurrent AOD records with UVI and TOZ measurements.

Concerning UVI_{fun}, it can be concluded that it offers very good results even though it considers aerosols implicitly. Nevertheless, this is not too much surprising because this algorithm was derived using some of measurements considered here.

6 Conclusions

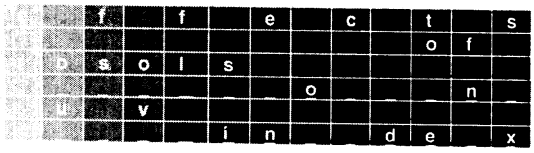

This work has presented a sensitivity study of the aerosol parameters concerning their effect on UVI, and has developed a parameterisation to explain the relative effect of aerosols on UVI. It has proposed an algorithm to fully calculate UVI for a wide range of situations; a first test of validation with measurements has also been presented.
After all these analyses, this Chapter summarizes the main results found and recommends future studies to continue this work.

6.1 Conclusions ←

In the following, we summarize the results obtained for each of the issues treated.

Sensitivity study

- The effect of aerosols on UVI has been found to be almost independent of TOZ, which has allowed us to study the aerosols effect independently of the ozone effect.
- SZA plays an important role in the explanation of the effect of aerosols. We have found angular dependence up to 6% and 4% (from 0 to 60 degrees) in the effect of AOD_{368} and SSA, respectively. For G and alpha it is much weaker.
- As expected, AOD_{368} is the most important parameter to explain the aerosols effect on UVI, with a maximum absolute effect of 6. SSA has been found to play an important role with a maximum absolute effect of 2.8.
- G and alpha are much less important parameters and their maximum absolute effect on UVI is ±0.8. If these two parameters are set at the considered reference values (G=0.7 and alpha=1.4) maximum uncertainties in UVI are ±0.4.
- These results have made us decide to consider AOD_{368}, SSA and SZA in the aerosols effect parameterisation.

Aerosol relative effect parameterisation

- We have seen that the relative aerosol effect on UVI can be well explained using the exponential expression $e^{-b(SZA,SSA)\,AOD_{368}}$.
- Fits have always regression coefficients greater than 0.99.
- For a wide range of conditions, the parameterisation has maximum relative and absolute errors of ±3% and ±0.2, respectively, in comparison with the TUV model calculations.

UVI algorithms

- We estimate that UVI_{fun} implicitly considers an AOD_{368} of about 0.3 with SSA=0.9. Considering this aerosol conditions, the comparison of UVI_{fun} with the TUV model has resulted in relative differences in UVI from +4% and -27% and absolute deviations between -0.61 and 0.54. Quite different TOZ dependencies have been found for both calculations.

- A TUV-based UVI algorithm (UVI_{fituv}) has been derived using the same kind of expression than UVI_{fun} and including the aerosol parameterisation. It considers 4 main parameters: SZA, TOZ, AOD_{368} and SSA. This parameterisation has theoretical maximum relative errors (in comparison with TUV) of –8% and +6% and absolute errors of ±0.4.
- A first test to validate UVI_{fun} has been presented with 4 years of measurements in De Bilt. Results found are not better than if we use UVI_{fun}. Limitations have been detected in the dataset of measurements used; the most important one is likely the lack of concurrence between the UVI and AOD_{368} measurements.

As a final conclusion, we can affirm that the objective of this work has been accomplished in the sense that a parameterisation to explain the effect of aerosols has been found and an algorithm to calculate UVI has been proposed with low errors for a wide range of conditions. Nevertheless, we don't know yet the practical utility of this formula, most of all because accurate input parameters are necessary. Further analyses are needed to understand better the results found in the validation test but also another dataset should be found in order to validate UVI_{fituv}, with UVI measurements for larger ranges of SZA, TOZ and with aerosol data concurrent with them.

7 Appendix

Effects of aerosols on uv index

Here we present in graphics the results of the sensitivity study made for the four aerosol parameters considered in the TUV model: Single scattering albedo (SSA), asymmetry factor (G), Ångström parameter (alpha) and the aerosol optical depth at 368 nm (AOD_{368}). Representations of the ratio and difference between each case considered and the reference case (see table 32) are shown. See Chapter 3 for explanations about the figures and further information about the sensitivity study.

SSA 0.9

0.6 0.65 0.7 0.75 0.8 0.85 0.95 1.0

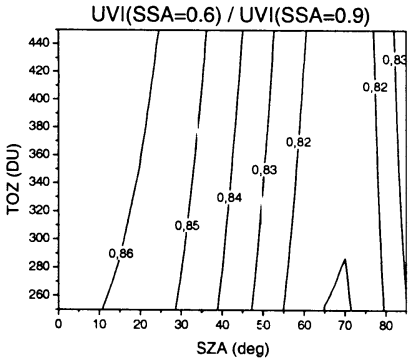

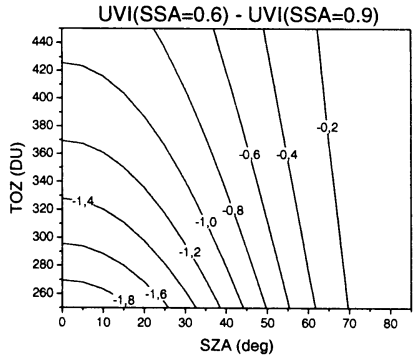

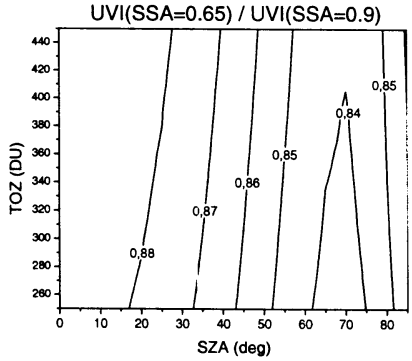

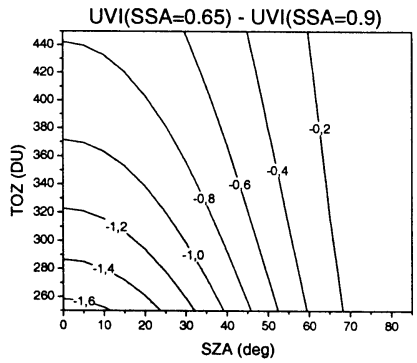

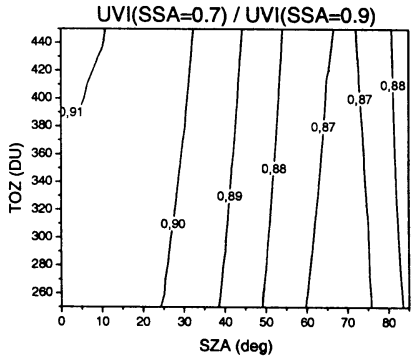

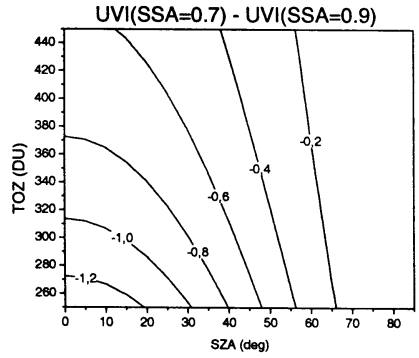

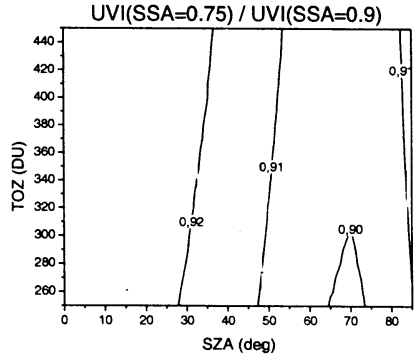

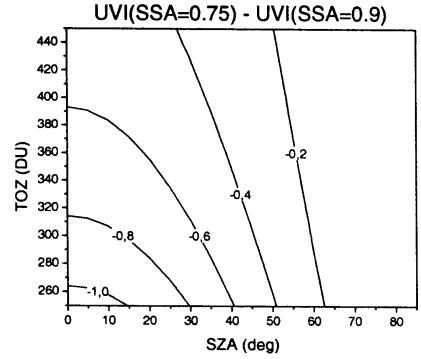

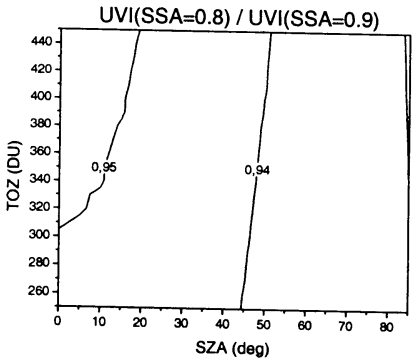
UVI(SSA=0.8) / UVI(SSA=0.9)
TOZ (DU)
SZA (deg)
0,95
0,94

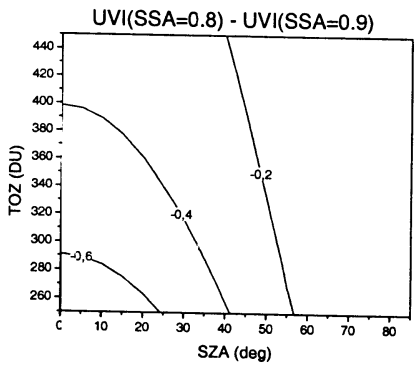
UVI(SSA=0.8) - UVI(SSA=0.9)
TOZ (DU)
SZA (deg)
-0,2
-0,4
-0,6

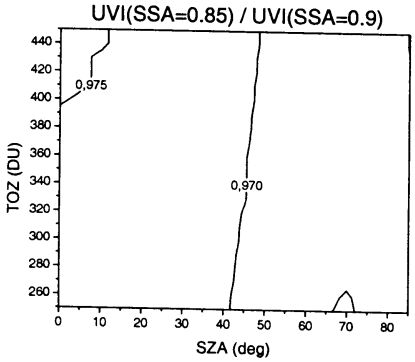
UVI(SSA=0.85) / UVI(SSA=0.9)
TOZ (DU)
SZA (deg)
0,975
0,970

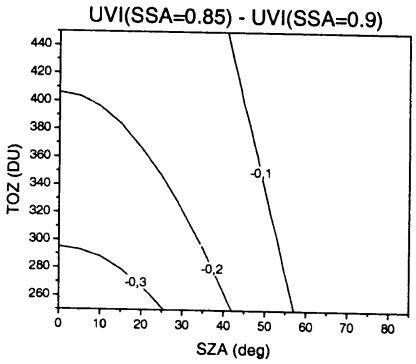
UVI(SSA=0.85) - UVI(SSA=0.9)
TOZ (DU)
SZA (deg)
-0,1
-0,2
-0,3

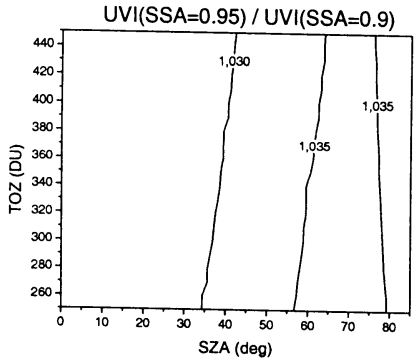
UVI(SSA=0.95) / UVI(SSA=0.9)
TOZ (DU)
SZA (deg)
1,030
1,035
1,035

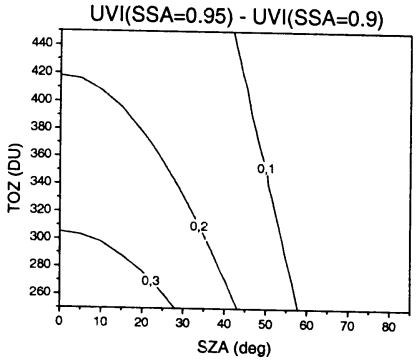
UVI(SSA=0.95) - UVI(SSA=0.9)
TOZ (DU)
SZA (deg)
0,1
0,2
0,3

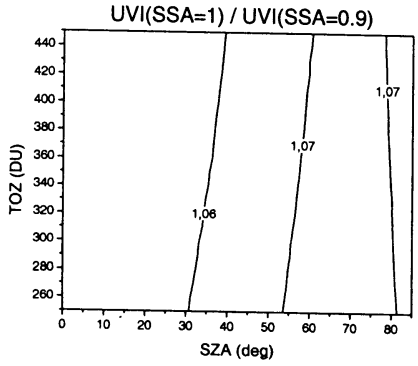
UVI(SSA=1) / UVI(SSA=0.9)
TOZ (DU)
SZA (deg)
1,06
1,07
1,07

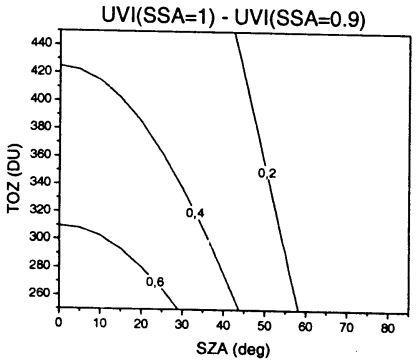
UVI(SSA=1) - UVI(SSA=0.9)
TOZ (DU)
SZA (deg)
0,2
0,4
0,6

G 0.7

0.5 0.6 0.8 0.9

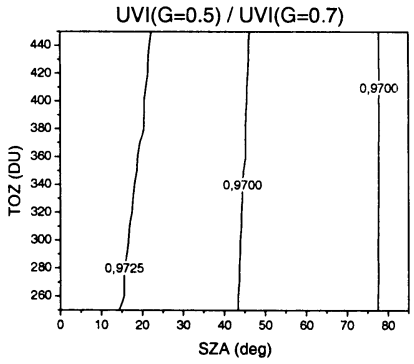

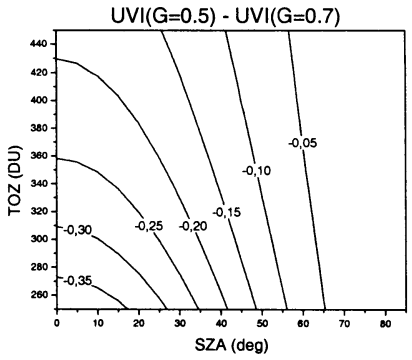

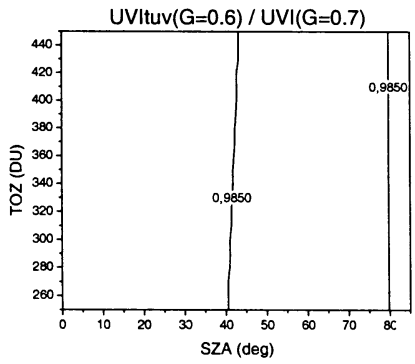

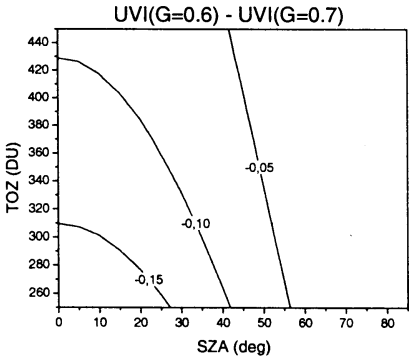

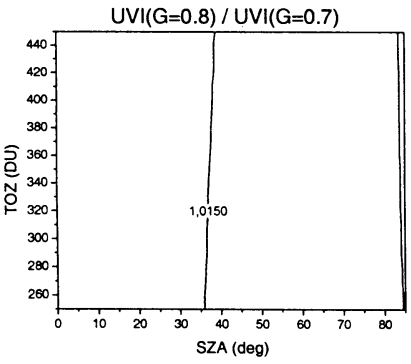

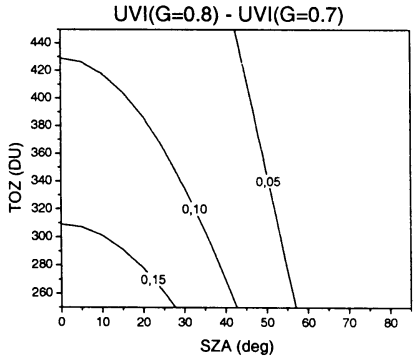

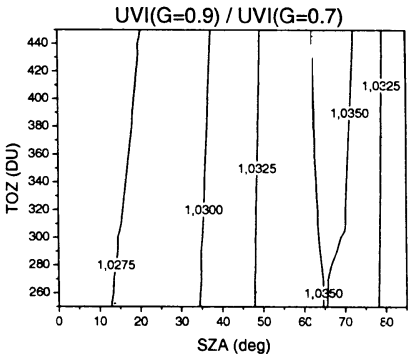

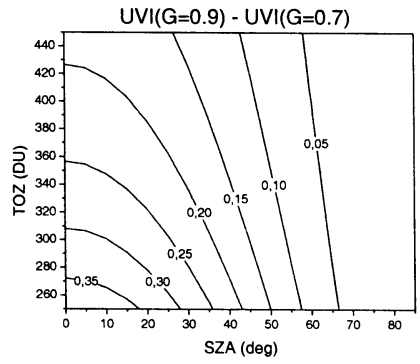

alpha 1.4

0 0.4 0.9 1.9 2.4 2.9

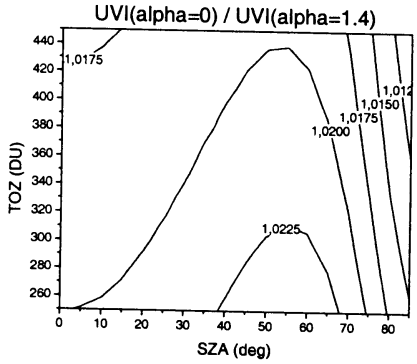

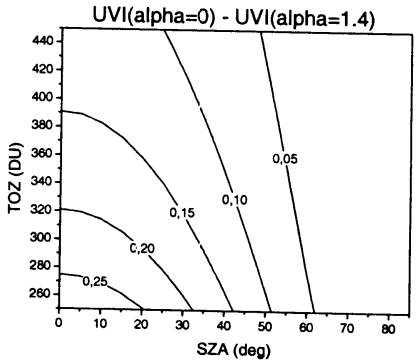

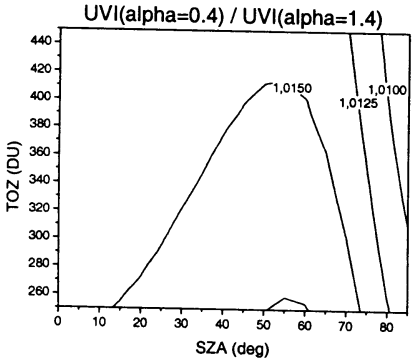

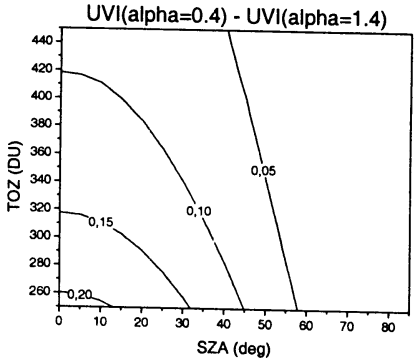

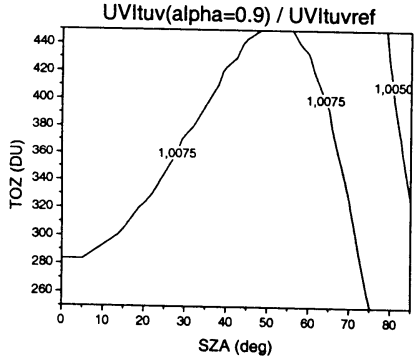

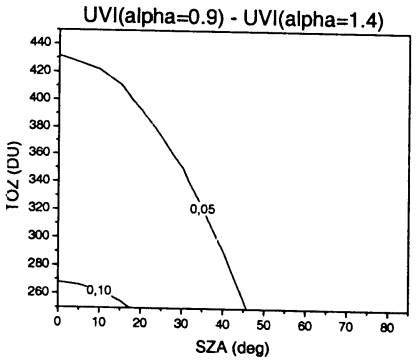

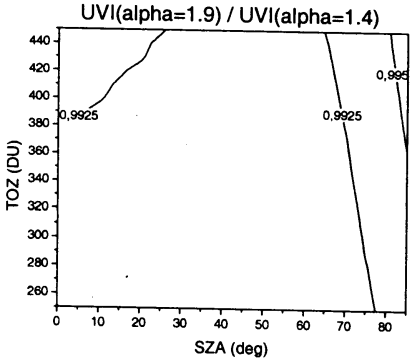

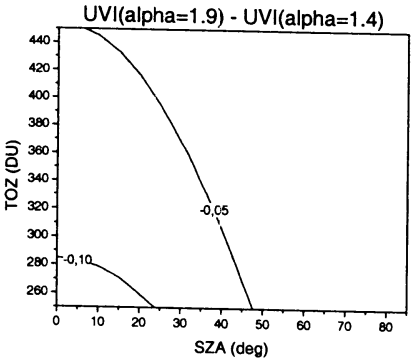

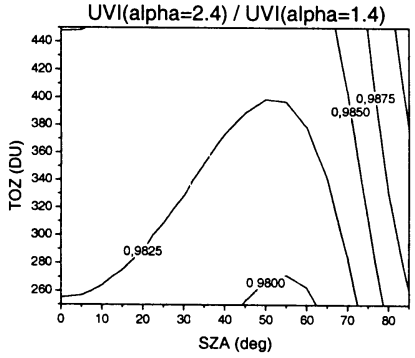

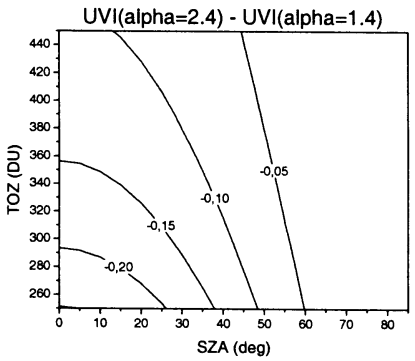

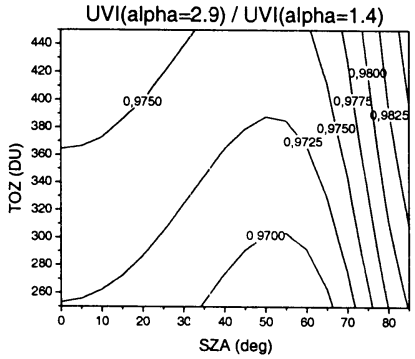

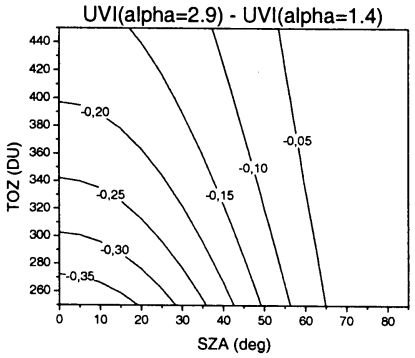

AOD(368nm) 0.3

0 0.1 0.2 0.4 0.5 0.6 0.7 1.0 1.2 1.5

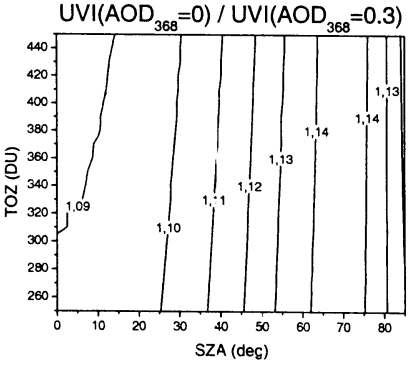

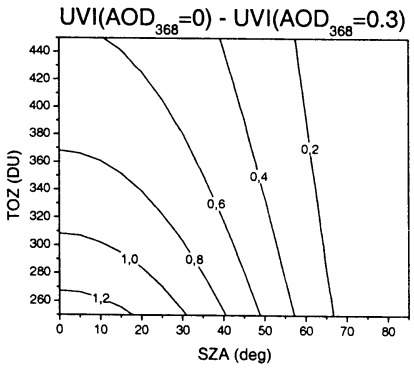

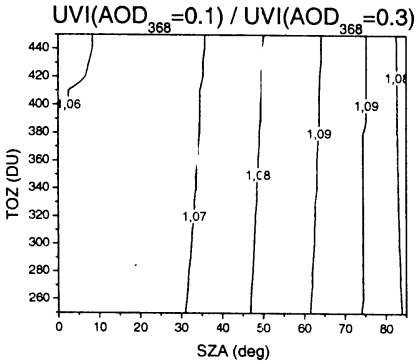

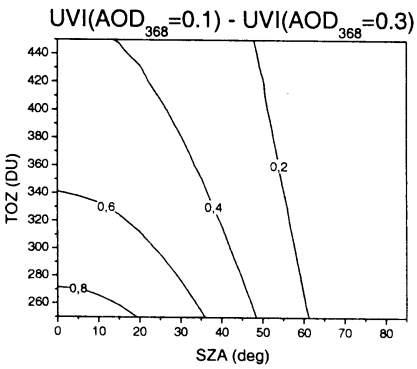

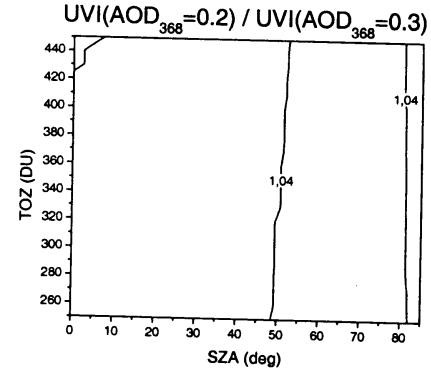
UVI(AOD368=0.2) / UVI(AOD368=0.3)
TOZ (DU)
SZA (deg)
1,04
1,04

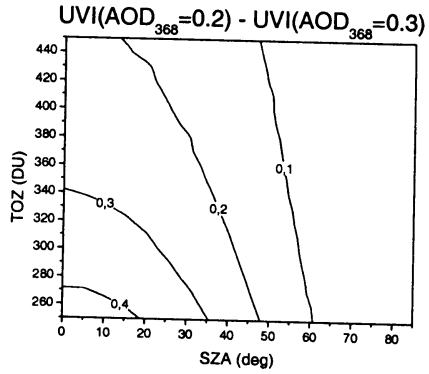
UVI(AOD368=0.2) - UVI(AOD368=0.3)
TOZ (DU)
SZA (deg)
0,1
0,2
0,3
0,4

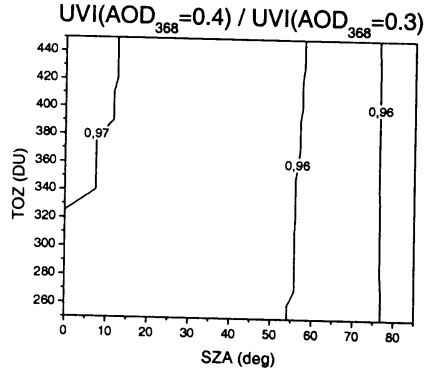
UVI(AOD368=0.4) / UVI(AOD368=0.3)
TOZ (DU)
SZA (deg)
0,97
0,96
0,96

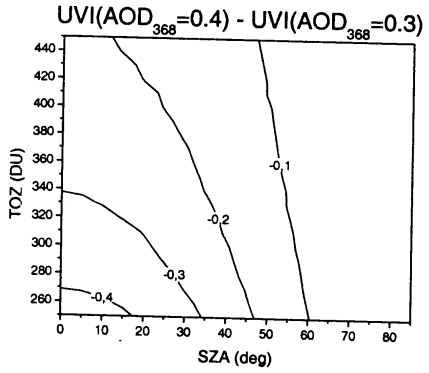
UVI(AOD368=0.4) - UVI(AOD368=0.3)
TOZ (DU)
SZA (deg)
-0,1
-0,2
-0,3
-0,4

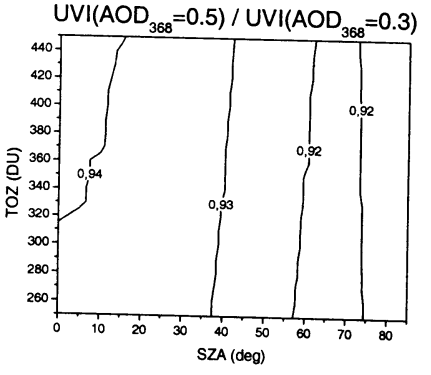
UVI(AOD368=0.5) / UVI(AOD368=0.3)
TOZ (DU)
SZA (deg)
0,94
0,93
0,92
0,92

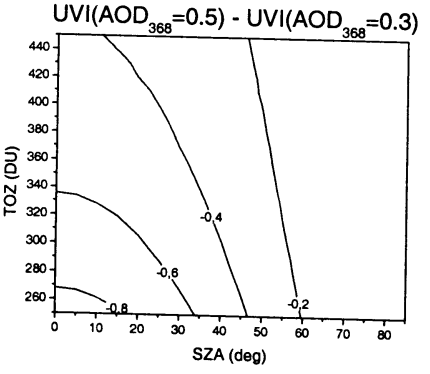
UVI(AOD368=0.5) - UVI(AOD368=0.3)
TOZ (DU)
SZA (deg)
-0,2
-0,4
-0,6
-0,8

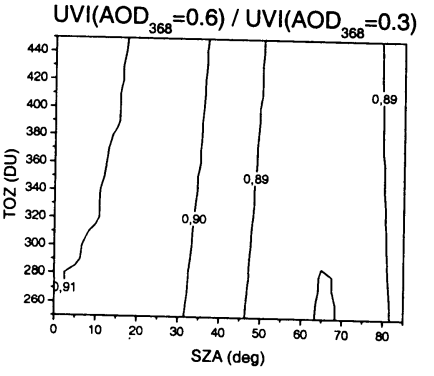
UVI(AOD368=0.6) / UVI(AOD368=0.3)
TOZ (DU)
SZA (deg)
0,91
0,90
0,89
0,89

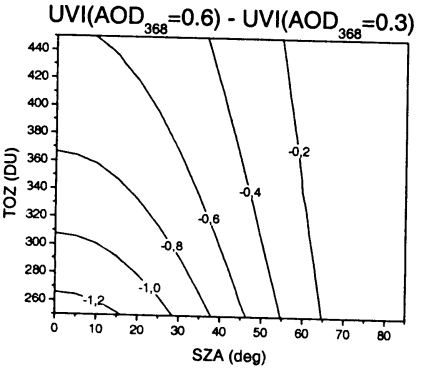
UVI(AOD368=0.6) - UVI(AOD368=0.3)
TOZ (DU)
SZA (deg)
-0,2
-0,4
-0,6
-0,8
-1,0
-1,2

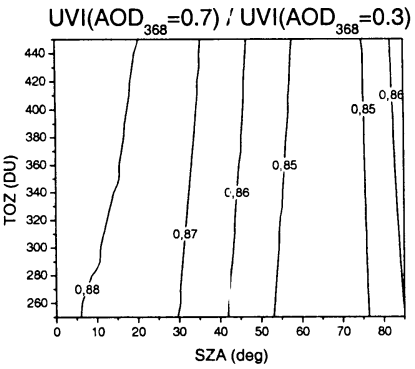
UVI(AOD368=0.7) / UVI(AOD368=0.3)
TOZ (DU)
SZA (deg)
0,88
0,87
0,86
0,85
0,85
0,86

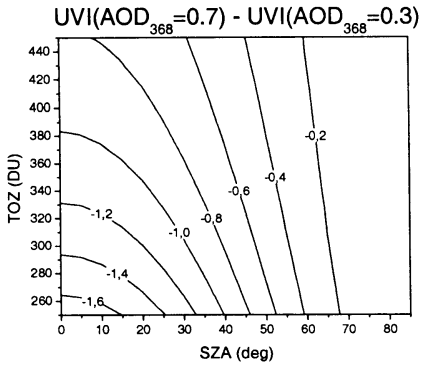
UVI(AOD368=0.7) - UVI(AOD368=0.3)
TOZ (DU)
SZA (deg)
-0,2
-0,4
-0,6
-0,8
-1,0
-1,2
-1,4
-1,6

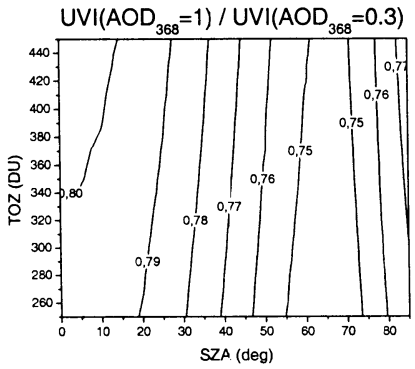
UVI(AOD368=1) / UVI(AOD368=0.3)
TOZ (DU)
SZA (deg)
0,80
0,79
0,78
0,77
0,76
0,75
0,76
0,77

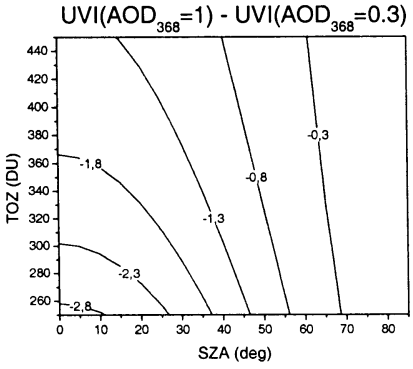
UVI(AOD368=1) - UVI(AOD368=0.3)
TOZ (DU)
SZA (deg)
-0,3
-0,8
-1,3
-1,8
-2,3
-2,8

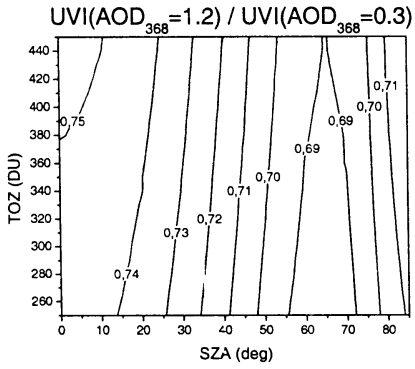
UVI(AOD368=1.2) / UVI(AOD368=0.3)
TOZ (DU)
SZA (deg)
0,75
0,74
0,73
0,72
0,71
0,70
0,69
0,69
0,70
0,71

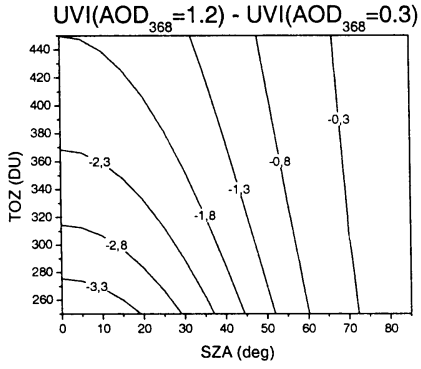
UVI(AOD368=1.2) - UVI(AOD368=0.3)
TOZ (DU)
SZA (deg)
-0,3
-0,8
-1,3
-1,8
-2,3
-2,8
-3,3

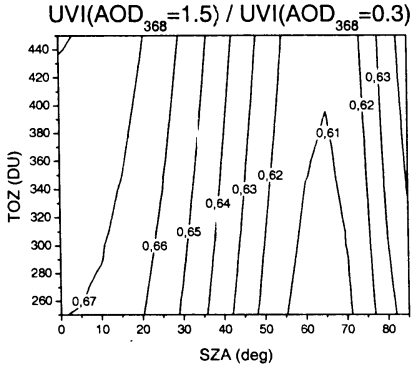
UVI(AOD368=1.5) / UVI(AOD368=0.3)
TOZ (DU)
SZA (deg)
0,67
0,66
0,65
0,64
0,63
0,62
0,61
0,62
0,63

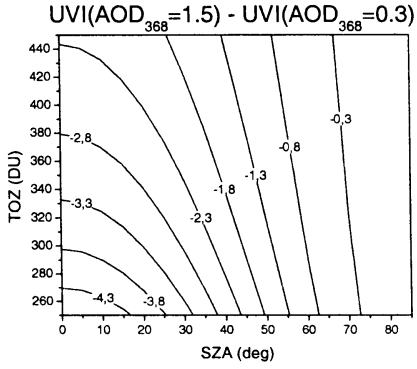
UVI(AOD368=1.5) - UVI(AOD368=0.3)
TOZ (DU)
SZA (deg)
-0,3
-0,8
-1,3
-1,8
-2,3
-2,8
-3,3
-3,8
-4,3

8 References

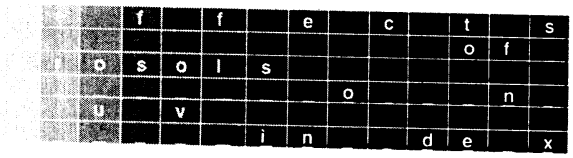

Allaart M., van Weele M., Fortuin P., Kelder H. (2002) "UV-index as a function of Solar Zenith Angle and Total Ozone" Submitted to *Meteorological Applications*

Ångström A. (1961) "Techniques of determining the turbidity of the atmosphere" *Tellus* 13, 214-223

Badosa J. (2002) "*Mesures d'Irradiancia eritematica a Catalunya vs modelitzacions per cels serens a partir de la columna d'ozo d'EP/TOMS*" Minor Thesis. University of Girona. Available at the web site: http://copernic.udg.es/angelets/jordi/treballderecerca.pdf

Cachorro V.E., González M.J., De Frutos A.M., Casanova J.L. (1989) "Fitting Ångström's formula to spectrally resolved aerosol optical thickness" *Atmospheric Environment* 23 (1), 265-270

Hänel G. (1994) "Optical properties of atmospheric particles: complete parameter sets obtained through photometry and an improved inversion technique" *Applied Optics* 33 (30), 7187-7199

Iqbal M. (1983) "An introduction to solar radiation" *Academic, New York*

Koepke P., Bais A., Balis D., Buchwitz M., De Backer H., de Cabo X., Eckert P., Eriksen P., Gillotay D., Heikkilä A., Koskela T., Lapeta B., Litynska Z., Lorente J., Mayer. B., Renaud A., Ruggaber A., Schauberger G., Seckmeyer G., Seifert P., Schmalwieser A., Schwander H., Vanicek K., Weber M. (1998) "Comparison of models used for UV Index calculations" *Photochemistry and Photobiology* 67 (6) 657-662

Krupa S.V., Kickert R.N., Jäger H.J. (1998) "Elevated Ultraviolet (UV)-B radiation and Agriculture" *Springer*

Lenoble J. (1993) "Atmospheric radiative transfer" *A. Deepak Publishing*

Liu S.C., McKeen S.A., Madronich S. (1991) "Effect of anthropogenic aerosols on biologically active ultraviolet radiation" Geophysical Research Letters 18 (12), 2265-2268

Long C.S., Miller A.J., Lee H.T., Wild J.D., Przywarty R.C., Hufford D. (1996) "Ultraviolet Index forecasts issued by the National Weather Service" *Bulletin of the American Meteorological Society* 77(4) 729-748

Lorente J., Redano A., De Cabo X. (1994) "Influence of urban aerosol on spectral solar irradiances" *Journal of Applied Meteorology* 33, 406-415

Madronich S. (1993) "The atmosphere and UV-B radiation at ground level" in *Environmental UV Photobiology*, edited by A.R. Young, Plenum, New York

Madronich S., Flocke S., Zeng J., Petropavlovskikh I., Lee-Taylor J. (2002) "Tropospheric Ultraviolet-Visible radiation model (TUV) version 4.1". Web page: http://www.acd.ucar.edu/TUV/

McKinlay A.F., Diffey B.L. (1987) "A reference action spectrum for ultraviolet induced erythema in human skin. In: Human exposure to ultraviolet radiation: Risks and regulations" *Passchier W. R., Bosnajakovich B.M.F. (Eds.)* (Amsterdam: Elsevier) 83-87

Meleti C., Capellani F. (2000) "Measurements of aerosol optical depth at Ispra: Analysis of the correlation with UV-B, UV-A, and total solar irradiance" *Journal of Geophysical Research D* 105 (4), 4971-4978

Renaud A., Staehelin J., Fröhlich C., Philipona R., Heimo A. (2000) "Influence of snow and clouds on erythemal UV radiation: Analysis of Swiss measurements and comparison with models" *Journal of Geophysical Research D* 105 (4) 4961-4969

Reuder J., Schwander H. (1999) "Aerosol effects on UV radiation in nonurban regions" *Journal of Geophysical Research D* 104 (4), 4065-4077

Sabburg J., Wong J. (2000) "The effect of clouds on enhancing UVB irradiance at earth's surface: A one year study" *Geophysical Research Letters* 27 (20) 3337-3340

Seckmeyer G. (2000) "Coordinated ultraviolet radiation measurements" *Radiation Protection Dosymetry* 91 (1-3) 99-103

Stammes P., Henzing J.S. (2000) "Multispectral aerosol optical thickness at De Bilt, 1997-1999" *Journal of Aerosol Science* 31, S283-S284 [Special Issue EAC 2000]

Tunc S. (1999) "Enhancement of solar and ultraviolet surface irradiance under partial cloudy conditions" *KNMI* (Scientific Report; WR 99-01)

Vanicek K., Frei T., Litynska Z., Schmalwieser A. (2000) "UV-Index for the public. A guide for publication and interpretation of solar UV Index forecasts for the public prepared by the Working Group 4 of the COST-713 Action "UVB Forecasting" COST-713. Available in the web site: http://www.lamma.rete.toscana.it/uvweb/

von Hoyningen-Huene W., Wendisch M. (1994) "Variability of aerosol optical parameters by advective processes" *Atmospheric Environment* 28 (5), 923-933

von Hoyningen-Huene W., Stettler M., Weller M. (1996) "Determination of climate-relevant aerosol parameters in the vicinity of an industrial regian in eastern Germany" Meteorologisch Zeitschrift N.F. 5, 269-278

Waggoner A. P., Weiss R.E., Ahlquist C., Covert D.S., Will S., Charlson R.J. (1981) "Optical characteristics of atmospheric aerosols" *Atmospheric Environment* 15 (10/11), 1891-1909

Weihs P., Rengarajan G., Simic S., Laube W., Mikielewicz W. (2000) "Measurements of the reflectivity in ultraviolet and visible wavelength range in a mountainous region" *Radiation Protection Dosimetry* 91 (1-3) 193-195

Wenny B. N., Saxena V. K., Frederick J. E. (2001) "Aerosol optical depth measurements and their impact on surface levels of ultraviolet-B radiation" Journal of Geophysical Research D 106 (15), 17311-17319

Ziemke J.R., Herman J.R., Stanford J.L., Bhartia P.K. (1998) "Total ozone/UVB monitoring and forecasting: Impact of clouds and the horizontal resolution of satellite retrievals" *Journal of Geophysical Research D* 103 (4) 3865-3871

Acknowledgments:

This work has been undertaken with the finacial support of:
Departament d"Universitats, Recerca i Societats de la Informació of the
Generalitat de Catalunya and the Netherlands Agency for Aerospace Programs (NIVR)

The work has been performed in the framework of the UV Index
SCIAMACHY validation project

The authors wish to thank Gerbrand Komen (HKS) and
Hennie Kelder (HAS) for their support to this work

I want to thank Piet Stammes and Marc Allaart for the use of their data and their advise and kind help in this work. I especially thank Michiel van Weele for the opportunity given and the attentions dedicated before and during my stage.

This has been much more than research, a unique life experience that leaves in memory an undeletable footprint.

Jordi.